COGNITIVE NEUROSCIENCE

Neuronal responses to omitted tones in the auditory brain: A neuronal correlate for predictive coding

Ana B. Lao-Rodríguez[1,2]†, Karol Przewrocki[3]†, David Pérez-González[1,2,4]†, Artoghrul Alishbayli[3], Evrim Yilmaz[3], Manuel S. Malmierca[1,2,5]*‡, Bernhard Englitz[3]*‡

Prediction provides key advantages for survival, and cognitive studies have demonstrated that the brain computes multilevel predictions. Evidence for predictions remains elusive at the neuronal level because of the complexity of separating neural activity into predictions and stimulus responses. We overcome this challenge by recording from single neurons from cortical and subcortical auditory regions in anesthetized and awake preparations, during unexpected stimulus omissions interspersed in a regular sequence of tones. We find a subset of neurons that responds reliably to omitted tones. In awake animals, omission responses are similar to anesthetized animals, but larger and more frequent, indicating that the arousal and attentional state levels affect the degree to which predictions are neuronally represented. Omission-sensitive neurons also responded to frequency deviants, with their omission responses getting emphasized in the awake state. Because omission responses occur in the absence of sensory input, they provide solid and empirical evidence for the implementation of a predictive process.

INTRODUCTION

Mismatch negativity (MMN) is a component of the auditory event–related potentials that is elicited when acoustic expectations are violated. It has been shown to correlate with behavioral and perceptual measures of deviance detection. Furthermore, the amplitude of the MMN response indexes the magnitude of the expectancy violation. The MMN response is widely considered as a neurophysiological correlate of a perceptual prediction error (*1*–*9*) that results from the comparison between the actual sensory (bottom-up) input and a memory trace, so-called prediction, encoded in top-down activity (*10*–*14*). A prediction error would arise when there is a mismatch between the internal prediction and the actual sensory input. A distinct aspect of the MMN is that the omission of an expected auditory stimulus (analogous to the deviant stimulus in an oddball paradigm) is often accompanied by elicitation of the omission MMN component in humans (*15*–*22*). This is important because it confirms that MMN is not simply a passive, bottom-up process that leads to synaptic adaptation to repeated stimuli due to a constant stimulation of the same afferent pathways (*8*, *23*). Previous studies have argued that the omission response provides conclusive, empirical evidence of the predictive process, as it occurs in the absence of sensory input (*19*, *20*).

Thus, predictions can be studied by examining the neuronal signature to the omission of an expected sound. Omission responses therefore might constitute a critical and underestimated test, particularly in animal models, which may be pivotal in uncovering the substrates of predictive processes. If stimulus-evoked neuronal activity indexes the difference between a sensory signal and its top-down prediction, then the omission of a predicted sensory signal should lead to neural activity, which reflects the pure prediction signal (*4*, *19*, *20*, *24*–*27*). A classic functional magnetic resonance imaging study has previously examined the topic of auditory imagery by introducing gaps of silence in familiar and unknown songs, showing neural activation of auditory cortex (AC) during the gaps of silence (*28*). However, empirical data at the single-neuron level in animal models to support the predictive coding hypothesis in this context are elusive.

We therefore aimed to investigate whether single neurons in different auditory areas respond to the omission of stimuli similar to the human MMN response. We used two rodent species that have proven to share a similar auditory system (*29*, *30*), which allow easy experimental manipulation in anesthetized or awake preparations. We found neural responses to the (silent) omission of a predictable pure tone in a subpopulation of neurons in the AC neurons under urethane anesthesia and in the awake state. In the latter, the proportion of AC neurons exhibiting omission responses was found to be substantially larger (~36% of recorded neurons, compared to 22% in anesthetized). These neurons responded to pure-tone stimuli but showed an even larger response when tones in a sequence of identical tones were omitted. We explored responses at different rates of tone trains and found that this distinct response to the omitted stimuli mostly occurred during rapid tone trains as in human MMN studies [stimulus onset asynchrony (SOA) $\leq$ 150 ms]. Omission selectivity increased during the sequence, primarily because of further adaptation of the response to the standard tone. In the awake state, omission responses became more distinct from deviant responses. Spatially, strong omission responses were more abundant in the caudal portions of the primary AC (A1), posterior auditory field (PAF), suprarhinal auditory field (SRAF), and ventral auditory field (VAF) in anesthetized rats.

[1]Cognitive and Auditory Neuroscience Laboratory (CANELAB), Institute of Neuroscience of Castilla y León, University of Salamanca, Salamanca, Spain. [2]Institute for Biomedical Research of Salamanca (IBSAL), Salamanca, Spain. [3]Computational Neuroscience Lab, Department of Neurophysiology, Donders Centre of Neuroscience, Nijmegen, Netherlands. [4]Department of Basic Psychology, Psychobiology and Methodology of Behavioral Sciences, University of Salamanca, Salamanca, Spain. [5]Department of Cell Biology and Pathology, University of Salamanca, Salamanca, Spain.
*Corresponding author. Email: msm@usal.es (M.S.M.); englitz@science.ru.nl (B.E.)
†These authors contributed equally to this work.
‡These authors contributed equally to this work.

RESULTS

Below, we first describe the quantitative characterization of omission-related responses and their dependence upon several experimental factors such as species, brain region, brain state, SOA, and sequence predictability. Then, we compare omission-related responses in relation to corresponding stimulus-bound (evoked) responses. Moreover, we investigate the latency of the responses, their sequence dependence, relation to pure-tone deviant responses, and their laminar and field specificity.

We tested whether neurons of the auditory pathway exhibit elevated responses to the omission of sounds within a fixed-rate, repetitive sequence, i.e., whether their response signifies a violated expectation of a regularly repeating sequence. For this purpose, we recorded neuronal activity in the AC of urethane-anesthetized rats (n = 77) and mice (n = 350) as well as awake mice (n = 393), and also from the inferior colliculus (IC) (n = 48; cf. Supplementary Materials) in urethane-anesthetized rats in response to a set of long pure-tone sound sequences. The sequences corresponded to an oddball paradigm (*31*) where the deviant was an omitted stimulus (Fig. 1 and fig. S1). We tested each neuron with a set of tone sequences, with fixed frequencies and intensities chosen to fall within its frequency response area. Sequences differed in their SOA (SOA: 125, 250, or 500 ms), in which the pre-activity and the analysis windows were chosen in accordance to the increasing SOAs to capture possible long latencies, and precise sequencing, either with a random number of tones before an omission or a fixed number (periodic). In a subset of the recordings in the mouse AC, we also presented classical oddball sequences of identical temporal structure with pure-tone deviants.

Omission responses were defined as a temporally localized elevation of spiking activity occurring during the periods of silence (omitted deviant; Fig. 1, asterisks in AC recording trace) when a stimulus was omitted (randomly or periodically, 10% probability in both cases) in a long sequence of tones (Fig. 1). Significance was assessed on a neuron level first before aggregating across neurons. This is essential as the classical theory of predictive coding (*14*) suggests that only a subset of neurons will respond to the omission of a predictable stimulus, likely signaling a prediction or prediction error (see Discussion for details), particularly inhibitory neurons (*19*–*21*). Specifically, we compared the neuronal activity recorded just before each omission trial (time windows of −25 to 5, −75 to 5, and −195 to 5 ms), with the window corresponding to the timing of the expected stimulus (5 to 120, 5 to 150, and 5 to 225 ms, respectively), using one-sided Wilcoxon signed-rank test at a

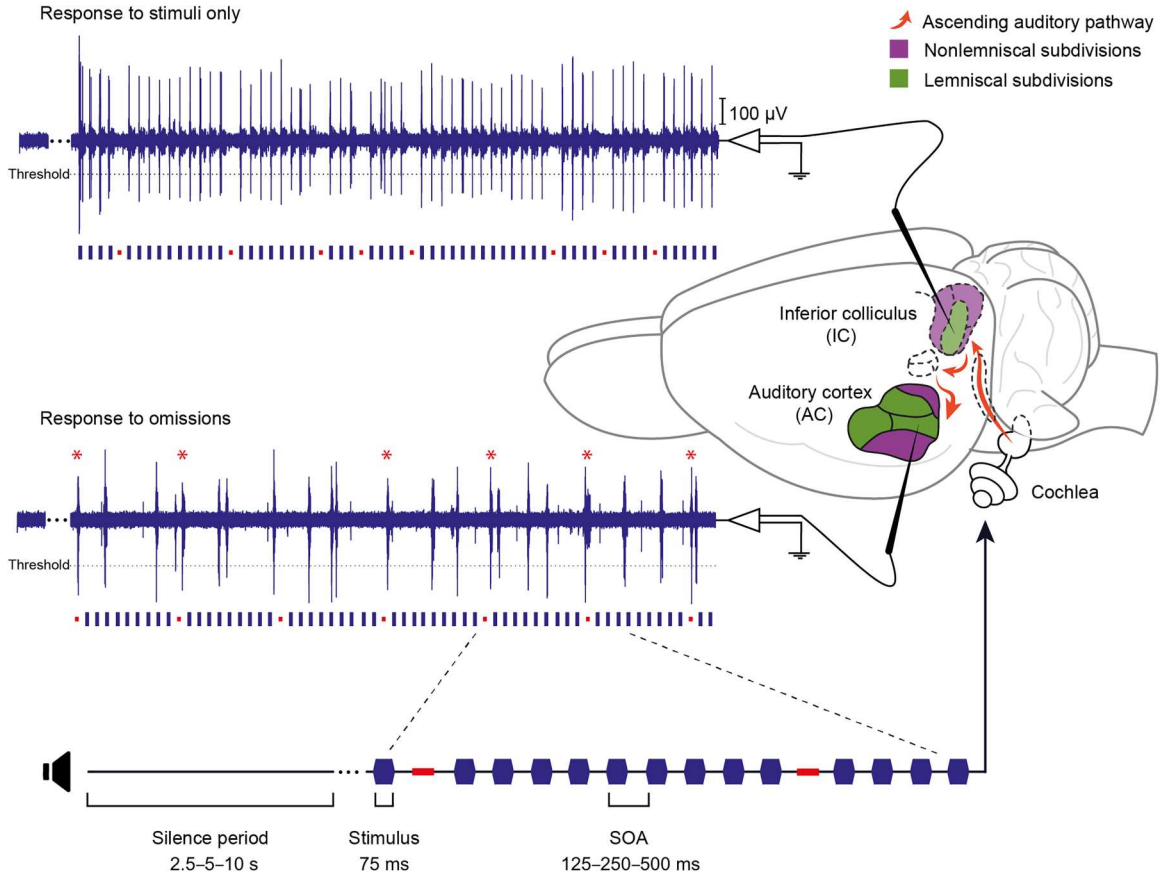

Fig. 1. Experimental setup and design for recording from the IC and AC. While stimulating with sequences of pure tones, neuronal activity was recorded using microelectrodes in the urethane-anesthetized rats (AC and IC) as well as urethane-anesthetized and awake mice (AC). The long tone sequence consisted of a repeating tone (standard probability: 90%) that was occasionally replaced by an omitted tone (average deviant probability: 10%). Traces correspond to actual recordings (from the IC and AC of urethane-anesthetized rats, respectively). Red stars indicate neuronal responses during an omitted tone. SOA denotes the amount of time between the start of one stimulus and the start of the following stimulus.

significance level of 0.05. We only checked for elevations in firing rate here, while we do not exclude that other neurons might show systematic reductions of their activity. To preempt a positive detection bias due to circular analysis ("double dipping") (*32*, *33*), we implemented split data analysis, i.e., half of the omission trials were used to assess whether a neuron showed a significant response, and the other half of the data were then used further on. In this way, random elevations of firing rate cannot systematically influence all subsequently analyzed measures. Following these criteria, 19.5% (15 of 77) and 21.7% (76 of 350) neurons from urethane-anesthetized rat and mice, respectively, as well as 35.6% (140 of 393) neurons from awake mice responded to omitted tones in 125 ms of SOA and are referred to as "omission-sensitive neurons." Data from the IC are only reported in the Supplementary Materials (cf. fig. S2), as the number of omission-sensitive neurons was too low for subsequent analyses.

Evidence of omission responses in AC neurons

Omission responses were originally found at an SOA of 125 ms in human electroencephalography (EEG) recordings (*16*). In the present experiments in rodents, we consistently find omission responses for this SOA (see Fig. 2A, red traces; representative neurons with significant omission responses, i.e., omission-sensitive neurons) under all three recording conditions. Omission responses in the AC of anesthetized rodents (Fig. 2A, left and middle) are salient in comparison to the preceding stimulus response, which is the last stimulus in the stimulation sequence before the omission. The omission response for the awake mouse AC neuron is very distinct, both in size and timing (Fig. 2A, right).

Next, we computed grand-average peristimulus time histograms (PSTHs) including all neurons showing significant omission responses (Fig. 2B; see Materials and Methods for details) for the three conditions. As in the individual cells, the omission responses are more robust as we progress from anesthetized to awake animals. Significantly, while positive omission responses are present in anesthetized rodents, AC populations (Fig. 2B, left and right), they are even more pronounced in the awake mouse preparation (Fig. 2B, right). The stimulus-evoked response (blue) shows less adaptation in awake mice (Fig. 2B, right) as opposed to cortical neurons in anesthetized rats and mice (Fig. 2B, left and middle). In awake mice, the onset responses to each stimulus are visible and the omission-evoked activity (red) is readily recognizable (Fig. 2B, right). The firing rate in response to sound stimulation is low in anesthetized rodents, except for the first stimulus after the omission, and it tends to increase during omitted tones (Fig. 2B, left and middle).

The shape of the responses to the stimulus typically had an onset component, both in individual examples and at the population level. Using the 115-ms analysis window that includes most of the evoked responses (see Materials and Methods), only in the case of the anesthetized animals the response to the stimulus after the omission was larger than the response to the stimulus previous to the omission ($P = 0.0125$ and $P < 0.0001$ for rats and mice, respectively; Wilcoxon test). However, when using a 30-ms analysis window encompassing only the onset component, we found that the response to the stimulus after the omission was larger than the response to the stimulus previous to the omission under all conditions (anesthetized rat: $P = 0.0496$, anesthetized mouse: $P = 0.0402$, awake mouse: $P < 0.001$; Wilcoxon test). Under the awake condition, as opposed to the responses to the stimuli, the omission responses tended to be more sustained and started from the expected time of occurrence of the omitted stimulus, often continuing to the subsequent stimulus presentation.

In summary, omission-evoked responses are strongly represented at 125 ms of SOA occurring both under anesthetized and awake states in the AC, with a substantial increase in magnitude in the awake state (for comparison with our smaller dataset from the IC, see fig. S2). At longer SOA (250 and 500 ms), we still detected a small subset of omission-sensitive neurons, but their average responses (based on the second half of the split data analysis) did not provide substantial evidence for reliable omission responses at these SOAs.

Table 1. Summary of firing rates.

Firing rates (spks/s)	AC anesthetized rat	AC anesthetized mouse	AC awake mouse
Mean			
Stimulus	1.0963	0.4046	2.0372
Omission	1.1347	1.0728	5.3385
After-omission	2.9421	3.1175	2.0246
Median			
Stimulus	0.8614	0.3840	1.4255
Omission	1.087	0.9116	3.2464
After-omission	1.1592	1.8439	1.8081
***P* values**			
Stimulus/pre-omission	0.0002	<0.0001	<0.0001
Omission/pre-omission	0.0001	<0.0001	<0.0001
After-omission/pre-omission	0.0001	<0.0001	<0.0001
Omission/stimulus	0.5765	0.0670	<0.0001
Stimulus/after-omission	0.0384	<0.0001	0.2756
Omission/after-omission	0.2769	0.0016	<0.0001

Comparison between sound and omission responses

Above, we identified putative omission-sensitive neurons using the split data approach on half of the omission trials. Below, we evaluate their response on the population level and compare them to responses to stimuli (not just the preceding one) and responses to stimuli after the omission. Each of these responses was referenced to the omission preceding activity to have a common local baseline, as we expect the spontaneous rate before the stimulation sequence to overestimate the within-sequence spontaneous rate (Wilcoxon test with Holm-Bonferroni correction, $P < 0.05$; Fig. 3). AC neurons from anesthetized rats and mice responded with similar firing rates to stimuli and omissions ($P = 0.577$ and $P = 0.067$, respectively; Fig. 3, A and B). On the other hand, awake mice AC neurons showed a significant enhancement of omission responses

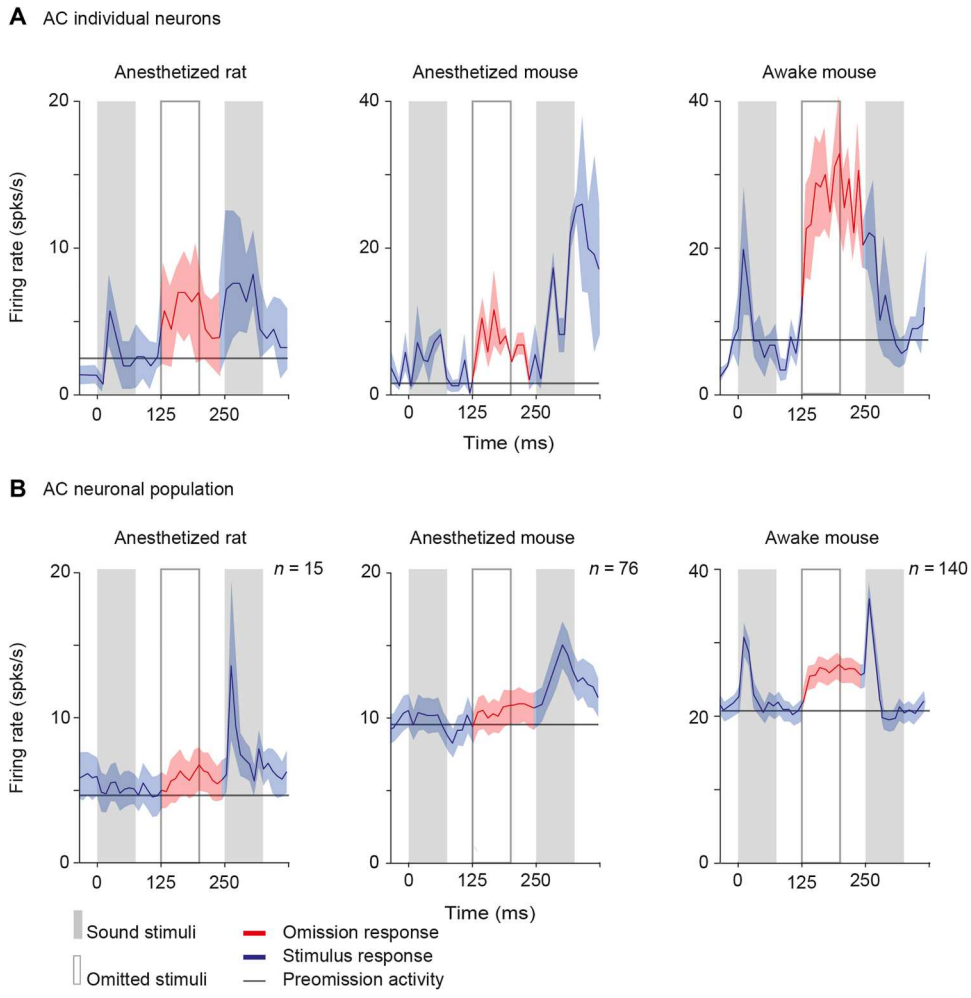

Fig. 2. Neurons in the AC show responses to the omission of a predictable sound. (**A**) Representative examples of omission responses in individual AC neurons. Neurons from the three recorded conditions are shown in the different columns (anesthetized rat, anesthetized mouse, and awake mouse; from left to right, respectively). Firing rates (spikes per second) and time (ms) are represented in vertical and horizontal axes. The duration of the stimuli and omitted tones (75 ms) is represented by vertical gray-shaded and white continuous line boxes, respectively. The responses have been computed as centered on the omitted tone whose response is occurring during the white vertical reference box. The red traces indicate responses during the omission analysis window. The preomission activity is also depicted as reference (gray horizontal line). Shaded areas indicate SEM. (**B**) Grand average of the responses of all the omission-sensitive neurons, per recorded condition, indicating the number of neurons included.

relative to stimulus responses ($P < 0.001$; Fig. 3C; cf. Table 1 for details).

We found that the response to the omission was particularly stronger than to the first stimulus after an omission under the awake condition, highlighting the omission response in the sequence ($P < 0.001$; Fig. 3C). The average firing rate in response to after-omission stimuli was significantly larger than the average response to the rest of stimuli in anesthetized rat and mouse neurons ($P = 0.038$ and $P < 0.001$), but not in awake mice AC neurons ($P = 0.276$), although it is also significant when using a 30-ms window, adapted to the brevity of the response (see above). The reduced average response to all stimuli (excluding after omissions) is probably due to an adaptation effect to the repeated stimuli (*7*, *34*), which is later released by the occurrence of the omission and subsequent after omission (see more details below in the "Omission-sensitivity dynamics depend on brain state" section).

Furthermore, we tested whether there were differences in the response to the omission under the periodic and random conditions (with a common, average probability for omissions of 10%), but there were no significant differences at the population level ($P = 0.93$, Wilcoxon test). As an occurrence of the omission in the periodic sequence is more predictable, we originally hypothesized a greater response under the random condition. The lack of a difference could be explained by the length of our shortest sequence under the random condition (*3*) in relation to the dynamics of response adaptation (see more details below in the "Omission-sensitivity dynamics depend on brain state" section and Discussion).

In summary, we find two important features regarding the omission firing rates: First, for omission-sensitive neurons, the firing rate during the omission is similar to the sound-evoked firing rate under the anesthetized condition (in both rat and mouse), but under the awake condition, the omission response is even larger than the

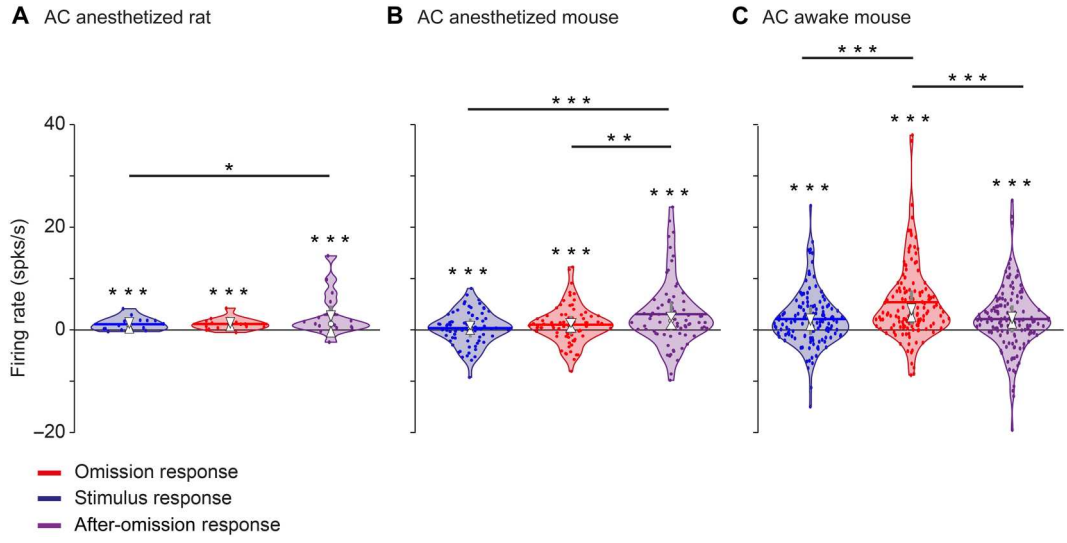

Fig. 3. The prevalence and strength of omission responses increase under awake condition. Firing rates of omission-sensitive neurons in the AC of the anesthetized rat (**A**), anesthetized mouse (**B**), and awake mouse (**C**). Sound-, omission-, and after-omission–evoked activities are represented by blue, red, and purple violin plots, respectively. In this and similar violin plots, the horizontal solid lines indicate the mean of the distribution, while the inner gray box indicates the interquartile range. Similarly, the white circles indicate the median and the white triangles show the 95% confidence interval for the median. Evoked firing rates have been baseline-corrected, relative to preomission activity. Asterisks directly over the violin plots indicate that the distribution is statistically different from 0 (Wilcoxon test with Holm-Bonferroni correction; see Table 1). Asterisks over horizontal lines indicate significantly different distributions (Wilcoxon test with Holm-Bonferroni correction; see Table 1). *$P < 0.05$, **$P < 0.01$, and ***$P < 0.001$.

sound-evoked activity over the analysis window. Second, the neural response of omission-sensitive neurons exhibits a timed rise at the start of the expected tone following an omission.

To quantify the comparison between sound- and omission-evoked activities, we computed an omission index (iOmi) at the cellular level [iOmi = (Omi FR − Stim FR)/(Omi FR + Stim FR)], for the omission-sensitive neurons, under the three recorded conditions, where the firing rate (FR) for stimuli was averaged from all stimulus presentations (Fig. 4A). Negative and positive iOmi values show neurons that exhibit a larger response to the sound or to the omission, respectively.

The average iOmi (Fig. 4A, vertical red dotted lines) quantifies the response selectivity to omissions for a group of neurons, here applied to the omission-sensitive neurons. Anesthetized rat AC neurons respond similarly on average to the stimulus and to the omission (iOmi = −0.089, $P = 0.661$, Wilcoxon test with Holm-Bonferroni correction; Fig. 4A, left), as well as anesthetized mouse AC neurons (iOmi = −0.006, $P = 0.836$; Fig. 4A, middle), while in awake mouse AC neurons, the average response to the omission is larger than to the stimulus (iOmi = 0.055, $P < 0.001$; Fig. 4A, right). Notably, the average iOmi is significantly larger in the awake mouse AC than in the anesthetized mouse AC ($P = 0.0013$, Wilcoxon rank sum).

Next, we compared the omission-sensitive (Fig. 4B, red) neurons to their complement, referred to as omission-insensitive (Fig. 4B, blue) neurons, in terms of the difference in activity to omissions and stimuli. In line with the definition of these groups of cells, we find that the omission-sensitive neurons have a larger difference than omission-insensitive neurons, thus relatively responding more to omissions ($P = 0.028$ and $P = 0.016$ for anesthetized rats and mice, respectively, and $P = 1.7 \times 10^{-8}$ for awake mice, Wilcoxon rank sum tests). While under urethane anesthesia, the difference is negative, i.e., greater responses to stimuli than to omissions, in both species (Fig. 4B); this relation reverses for the omission-selective neurons in the awake mouse (Fig. 4B, right, red). In all comparisons above, both omission and stimulus responses were referenced to the activity in the preomission period to focus on relative changes within cells instead of absolute firing rates.

In summary, the degree of omission selectivity in the neural responses was comparable between species in the AC and increased in the awake compared with the anesthetized state in the mouse. While omission selectivity differed in omission-sensitive and omission-insensitive populations under all conditions, the difference was most pronounced in the awake state.

Response latencies of omission and sound responses

To explore the omission responses further, we measured and compared the peak latency for the omission- and sound-evoked activity (paired Wilcoxon test with Holm-Bonferroni correction, $P < 0.05$; Fig. 5). Response latencies for omitted tones, stimuli, and after-omission stimuli are shown in Fig. 5 for the three recorded conditions. The neurons show very similar latencies for the omission- and stimuli-evoked responses in both anesthetized preparations (Fig. 5, A and B, and Table 2), while the latency of the omission responses is larger than the latency of the stimuli-evoked responses in the awake mouse AC ($P < 0.001$); this is probably caused by multiple factors, including differences in the profile of the responses to the stimulus (peaking closer to the sound onset) and the omission (more sustained responses), overall larger firing rates, and reduced stimulus adaptation under the awake condition, which would contribute to faster responses. A real and genuine omission response should be time-locked to the period when the stimulus is expected to happen (but it is omitted). These latency data support the notion that the source of the omission response (i.e., putative prediction)

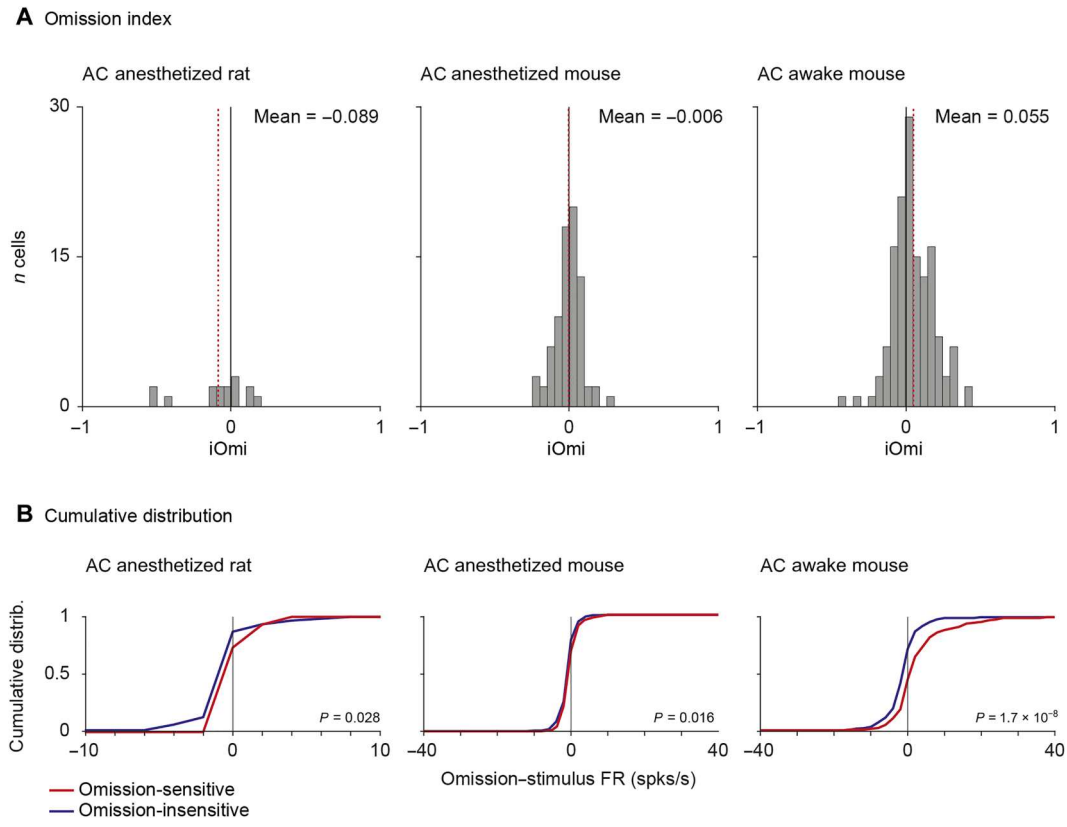

Fig. 4. Responses to omission become larger than stimulus responses under the awake condition. Distribution of iOmi between the recorded conditions. (**A**) iOmi for omission-sensitive neurons show progressively increasing values, from negative under the rat anesthetized condition, to positive values in the mouse preparations, being highest under the awake condition. Positive iOmi values indicate that the neuron responds with higher firing rates to the omission than to the stimulus, while negative values indicate the opposite. (**B**) Comparison of omission-sensitive (red) with omission-insensitive (blue) neurons shows increasing omission selectivity toward AC and further in the awake state. This is indicated by a larger separation between the curves, particularly for values >0, indicating greater responses to omissions than stimuli.

could differ from the stimulus response (forward response) as posited by predictive (*14*) coding (cf. Table 2 for details).

Comparison between omission and deviant responses

Responses to unexpected changes in tone properties, so called deviants, are very related to responses to omissions, as the latter can be considered a special case of a deviant. Their properties have long been studied under the topic of stimulus-specific adaptation—often considered a special case of predictive coding—where a certain degree of adaptation occurs for the repeated standard stimulus, while the deviant stimulus leads to a larger response, in higher auditory areas even larger than it would be in isolation (*7*, *8*, *10*, *23*, *34*). A natural question is whether the classical deviant responses co-occur with omission responses.

To address this question, we compare here the neural response for omission-sensitive neurons in the anesthetized and awake mouse AC (targeting A1). In the awake dataset, the deviant and omission conditions were presented for a subset of 126 (of a total of 393) cells, while in the anesthetized set, they were presented for all 350 cells, of which 55 and 76 were omission-sensitive, respectively. As usual, the deviant response (Fig. 6A, left column, orange) was larger than the standard response ($P = 1.4 \times 10^{-9}$, one-sided Wilcoxon signed-rank test; Fig. 6A, left column, blue), which, under the anesthetized condition, was nearly completely adapted. The omission response was less precisely timed than the deviant response, but was significantly larger than the preomission period (Fig. 6A, left, red). Under this condition, both omission-sensitive and omission-insensitive neurons responded similarly to omission and deviant stimuli, as evidenced by the overlap of the cumulative distributions of the difference between deviant and omission responses ($P = 0.15$, Wilcoxon rank sum test between the two populations on omission-deviant responses; Fig. 6A, middle and right). The curves intersect the ordinate at 0, indicating that responses to deviants were, on average, larger than to omissions.

On the other hand, the omission-sensitive neurons (Fig. 6B) also showed a very strong response to the deviant and a clearer response to the standard than under the anesthetized condition, likely because of reduced stimulus adaptation. In addition, the awake preparation shows a clear sustained response to the omission, with an overall rate similar to the deviant response ($P = 0.36$). Under this condition, omission-sensitive neurons respond to omissions with larger firing rates than to deviants ($P = 0.0017$), which is not the case for omission-insensitive neurons (Fig. 6B, middle). This is also indicated by the "dent" in the cumulative distribution of the difference between omission and deviant responses for the omission-sensitive neurons (Fig. 6B, right, red). These response

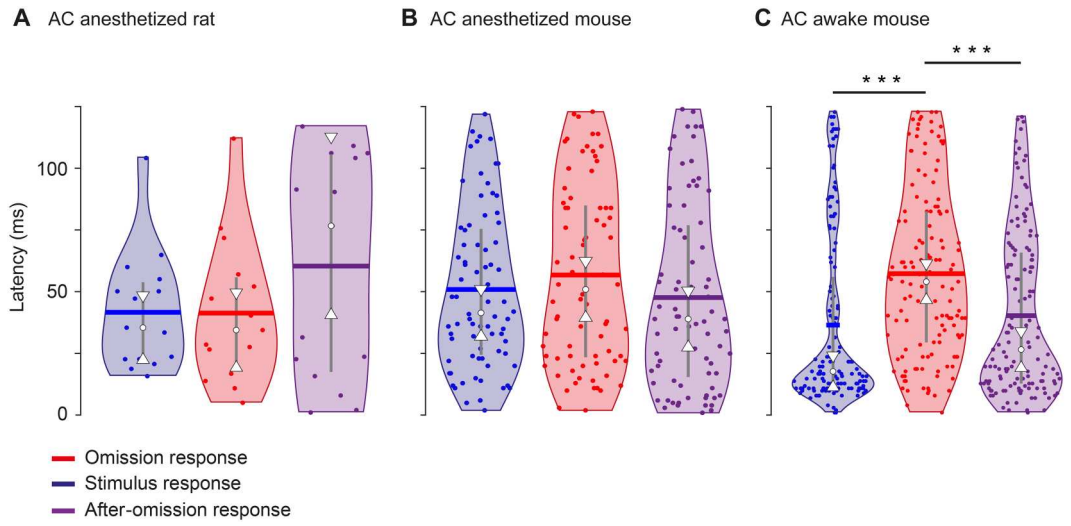

Fig. 5. Comparison of response latencies for omission and stimulus responses. Distribution of response peak latencies (ms) of omission-sensitive neurons in the AC of the anesthetized rat (**A**), anesthetized mouse (**B**), and awake mouse (**C**). The blue, red, and purple violin plots depict the distribution of the sound stimuli, omission, and after-omission latencies (see Fig. 3 for the meaning of the violin plot symbols). Asterisks denote statistical significance between stimuli and omission latencies (***P < 0.001; paired Wilcoxon with Holm-Bonferroni correction; see Table 2).

Table 2. Summary of responses latencies.

Response latency (ms)	AC anesthetized rat	AC anesthetized mouse	AC awake mouse
Mean			
Stimulus	42.8333	50.4474	36.5929
Omission	42.5	56.3289	57.8214
After-omission	61.9	47.1842	40.5
Median			
Stimulus	36.5	41	17.5
Omission	35.5	50.5	54.5
After-omission	78.5	38.5	26.5
***P* values**			
Stimulus/omission	0.8904	0.8904	<0.0001
Stimulus/after-omission	0.5830	0.5830	0.3066
Omission/after-omission	0.4052	0.4052	0.0001

properties in the AC show that omission-sensitive neurons can also have a response to deviant sounds; however, in the awake state, the omission response of the omission-sensitive neurons becomes comparable in size and more specific to omissions (see Discussion for details).

Omission-sensitivity dynamics depend on brain state

Next, we analyzed whether omission-sensitive neurons show a dependence of their response on the history of stimulation, and how this depends on the state of the animal. First, we considered the neural responses as a function of the overall stimulation sequence. As expected, the stimulus response exhibited a fast decay, within just two stimuli under both the anesthetized (Fig. 7A, left, blue) and the awake (Fig. 7A, right, blue) condition. Under the awake condition, a second time scale of adaptation existed with a time constant of ~5 s. The level of the omission responses (red) stayed rather constant over the period of the whole sequence in both states. The iOmi index of omission selectivity (Fig. 7B; see Methods) showed a slow increase, which was more pronounced under the awake case ($r = 0.39$, $P = 1.2 \times 10^{-16}$, Pearson correlation) than under the anesthetized condition ($r = 0.1$, $P = 0.035$). This was probably mostly driven by the adaptation of the standard response, potentially signifying a buildup of predictions (*21*).

Second, we studied the omission-evoked responses in relation to the number of stimuli preceding the stimulus omission. In the anesthetized case, a significant decrease [$P = 0.02$, Kruskal-Wallis analysis of variance (ANOVA)] is observed for the omission response (Fig. 7C, left, red). The response to the first standard after the omission (purple) shows a similar but nonsignificant dependence. Unexpectedly, no dependence with a decrease for shorter sequences of standards is present in the awake case (Fig. 7C, right); conversely, the standard response instead shows a significant decrease ($P = 0.00074$). For the omission response, no dependence is present, although the omission response is on a high level relative to the standards (firing rates are normalized to the average standard response here), which suggests that the omission response might already have reached a plateau level. This possibility is supported by the rapid adaptation of the standard response after the omission (Fig. 7D), which is very salient in the anesthetized case and completes after just two standard stimuli, and even after just one in the awake case. In the latter, this behavior is only apparent if a shorter time window (30 ms) is used for the analysis (Fig. 7D, right, inset), which matches the brief, driven response (see Fig. 2B, right).

In summary, the omission sensitivity shows a significant slow increase over prolonged stimulation, particularly under awake

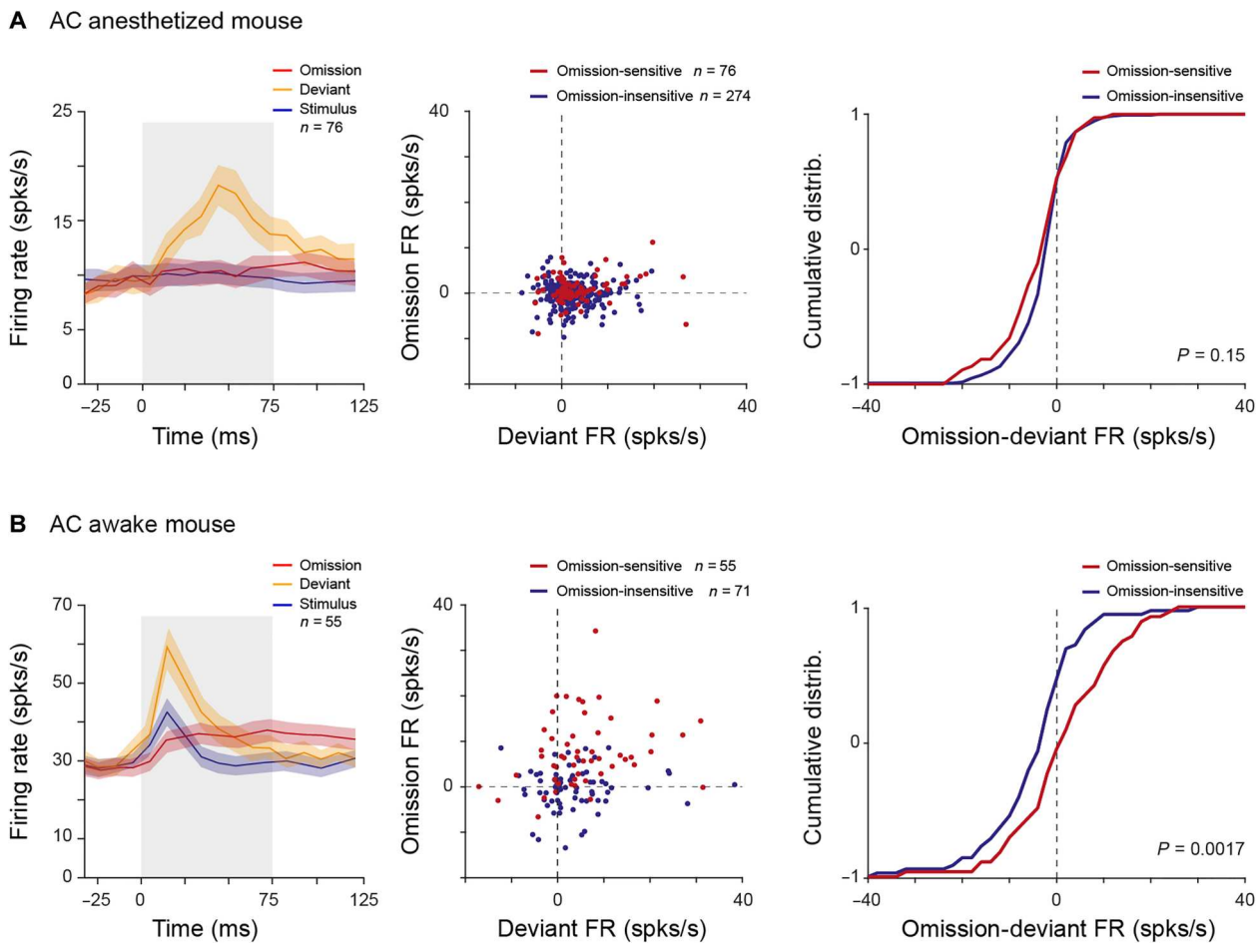

Fig. 6. Omission-sensitive neurons differentiate their response from deviants in the awake state. (**A**) In the AC in the anesthetized mouse, omission-sensitive neurons show a strong response to deviants (orange; left), which substantially exceed the omission (red) and standard stimulus (blue) responses [$P = 0.00018$ and $P = 1.4 \times 10^{-9}$, Wilcoxon signed-rank test (one-sided) between deviant responses relative to omission or standard responses; $n = 76$]. The relative responses of omission-sensitive (red) and omission-insensitive (blue) neurons to omissions and deviant stimuli are statistically indistinguishable (middle), indicated by the overlapping cumulative distributions of difference between omission and deviant responses (right column; $P = 0.15$, Wilcoxon rank sum test between the two populations on omission-deviant responses). Shaded areas in the left column indicate one SEM. All responses are relative to the preomission baseline period. (**B**) In the AC of the awake mouse, the responses are generally larger and the omission response becomes comparable in overall rate to the deviant response ($P = 0.36$), while the deviant response is ~91% larger than the stimulus response ($P = 2.7 \times 10^{-7}$). Many cells, particularly from the omission-sensitive (red) group, show omission responses that are larger than the deviant response (middle; red dots above diagonal). In the awake state, omission-sensitive neurons show a clear and significant separation in the difference between omission and deviant responses ($P = 0.0017$).

conditions. A dependence on the number of preceding standards is found in anesthetized, but not in awake. The latter might indicate that the omission response has already reached a plateau, which we cannot resolve presently, as even shorter sequences of standards (1 to 2) would be required.

Histological distribution of omission responses

The histological analysis of the electrolytic lesions in the IC demonstrates that omission-sensitive neurons are located in the nonlemniscal IC (fig. S3). To test whether omission responses show any specific distribution across the AC fields and/or layers, we analyzed where neurons with omission responses were located in the different AC regions (Fig. 8 and fig. S4).

We analyzed the distribution of omission-sensitive neurons across layers (Fig. 8, A to C). In the AC of anesthetized rats, the proportions of omission-sensitive neurons were 7.1, 35, and 22% for supragranular, granular, and infragranular layers, respectively (Fig. 8A, burgundy bars relative to gray). In the AC of anesthetized mice, these proportions were 26% of the neurons in the supragranular layers that were omission-sensitive, 30% in the granular, and 19% in the infragranular (Fig. 8B, burgundy bars). For awake mice AC neurons, these proportions were 40, 38, and 34% for the supragranular, granular, and infragranular layers, respectively (Fig. 8C, burgundy bars). We performed bootstrapping analysis on all three recording sets, but only found a significant reduction relative to the distribution of expected counts in the supragranular layer ($P = 0.003$, based on 300,000 independent draws, and $P < 0.05$ significance bound), although there appears to be a tendency for a higher fraction of omission-sensitive cells in supragranular layers in the awake compared with the anesthetized mouse. However,

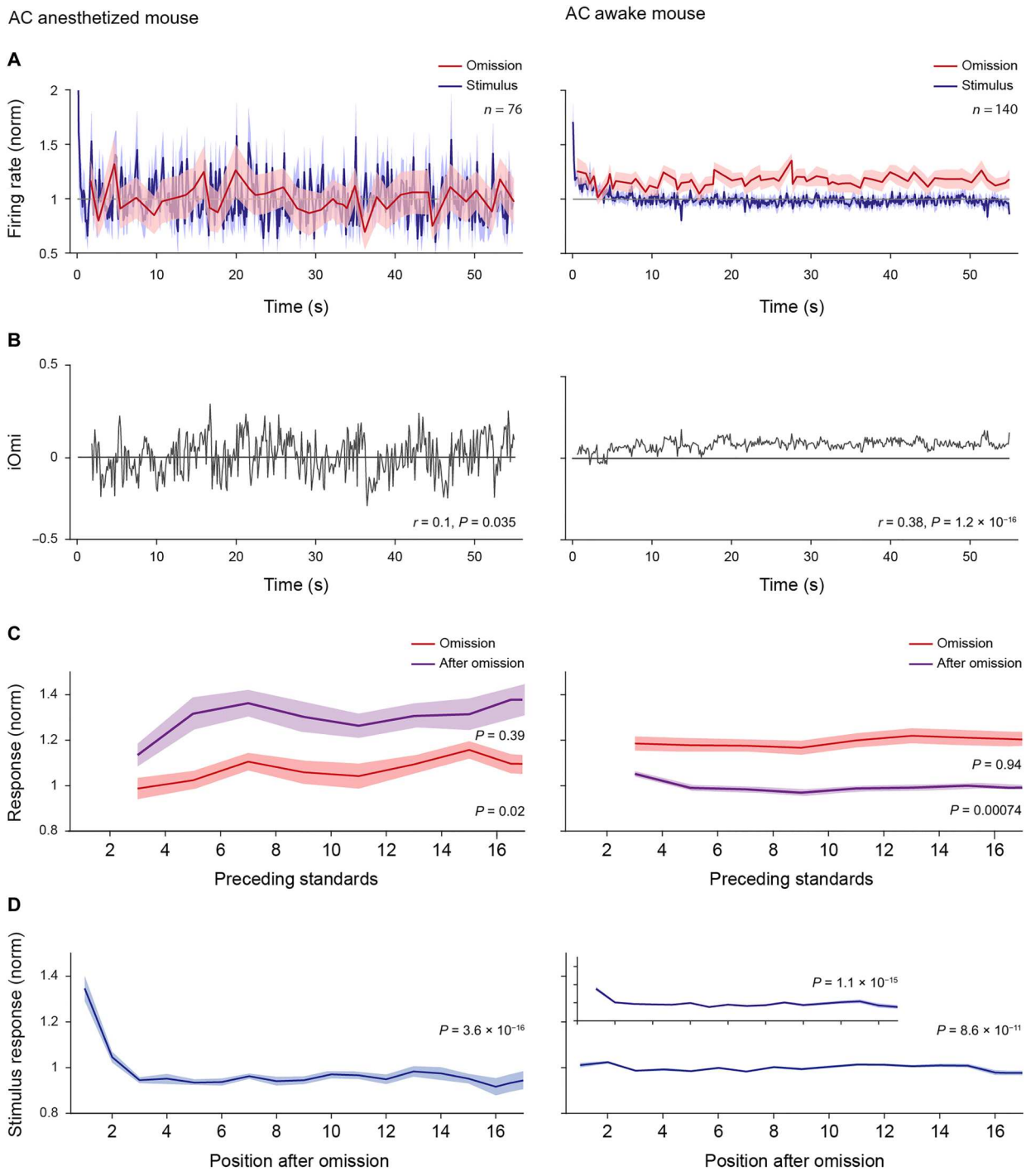

Fig. 7. Omission response progression depends on brain state. (**A**) Responses of the omission-sensitive cells to the standard stimulus (blue) adapt in both the anesthetized (left) and awake (right) state. Adaptation occurs more rapidly in the anesthetized state, reaching baseline already after ~1 s, while in the awake state, two time scales of adaptation are apparent, one very fast (one to two stimuli, i.e., ~125 to 250 ms) and the second with a time constant of ~5 s. The omission response stays rather constant over the entire period under both conditions but is consistently larger in the awake case ($P = 1.2 \times 10^{-22}$, Wilcoxon signed rank test between awake and anesthetized). (**B**) The index of omission sensitivity in relation to the standard responses, iOmi, consequently increases over time in the awake case ($r = 0.38$, $p = 1.2 \times 10^{-16}$, Pearson correlation), while this correlation is weaker and only borderline significant in the anesthetized case ($r = 0.1$, $P = 0.035$). (**C**) In the anesthetized state, the omission response exhibited a significant dependence on the number of standards preceding it [$P = 0.02$, Kruskal-Wallis analysis of variance (ANOVA)]. In the awake state, the omission response already starts at a high level and has no significant dependence on the number of preceding standards, possibly indicating that the dependence has already plateaued. The after-omission response shows a fast and significant decay to a plateau level. (**D**) The response to the standard following an omission decayed quickly, within two stimuli under anesthesia and just one stimulus in the awake (see inset for 20-ms analysis window; *P* values based on Kruskal-Wallis ANOVA). Using our standard analysis window (5 to 120 ms), the effect is also significant, but less pronounced, because of the brevity of the response (see Fig. 2B, right).

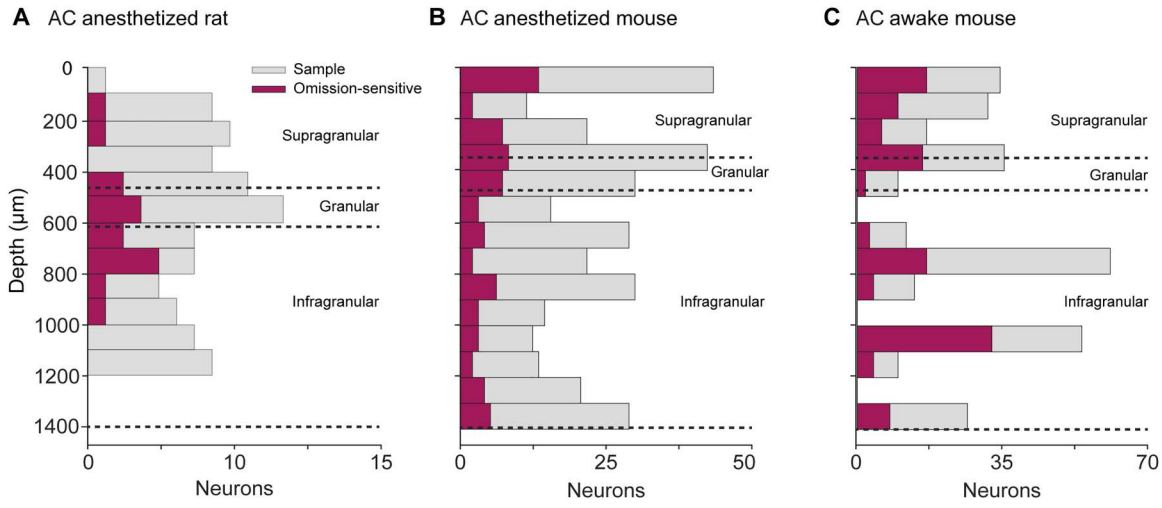

Fig. 8. Distribution of omission-sensitive neurons in the AC layers. (**A**) Anesthetized rat, (**B**) anesthetized mouse, and (**C**) awake mouse. Horizontal dashed lines indicate the boundaries between supragranular, granular, and infragranular layers. While the fraction of omission-sensitive neurons (burgundy bars) relative to the total sample (gray bars) is low in supragranular layers in anesthetized rats, for awake mice, there is a tendency toward a higher proportion of omission-sensitive neurons in the supragranular layers. Note that the depth AC is 1400 μm thick in mice because of the oblique trajectory of the recording electrodes to the pial surface, while in rat, it is 1200 μm thick because of the orthogonal trajectory.

additional research with higher-density probes will be required to fully address this question.

Last, we investigated the location of omission-sensitive neurons in subfields of the AC. Location data were only available in the rat, as the recordings in the mouse were all targeted toward A1 only. As we acknowledge that the number of cells is likely insufficient for a complete map, we provide these data in the supplement as suggestive evidence. To allocate each recorded neuron to a specific field in the rat AC, we recorded the frequency response areas and analyzed the topographical distribution of characteristic frequencies for all units. Each recording was assigned to a dorsoventral and rostrocaudal coordinate relative to bregma as in previous studies (*7*, *8*, *35*, *36*). This analysis allowed us to pool the data from all animals (fig. S4A) and construct a synthetic map of characteristic frequencies across the entire rat AC (*7*, *8*). Similar to these previous works, we found a high-frequency reversal zone between VAF (caudally) and anterior auditory field (AAF; rostrally), a low-frequency reversal zone between A1 and PAF (dorsocaudally), and a high-frequency reversal between VAF and SRAF (ventrally). Thus, we could reliably define the lemniscal (A1, AAF, and VAF) and nonlemniscal (SRAF and PAF) auditory cortical fields as shown in fig. S4A. The omission-sensitive neurons found in this study were located mostly toward the caudal areas of the AC, within the limits of A1, PAF, and SRAF (fig. S4A). When plotting iOmi levels for all significant sequences recorded (in this case, we did not use the average value per unit, because it would not allow to properly map the whole AC), it becomes evident that, although omission responses are distributed in all fields, the highest levels of iOmi were found in SRAF and PAF (fig. S4B).

DISCUSSION

The key finding of the current study is that a subset of neurons in the auditory brain responds to the absence of an expected stimulus, which provides empirical evidence in support of certain elements of predictive coding in a subcortical area and sensory cortex (*1*, *37*–*41*). Specifically, we demonstrate that robust neural activity emerges during the omission of a sound in a regular sequence of repetitive stimuli. These responses are consistent with prediction error signals, as these omissions result in the violation of an expected stimulus when it should occur. We identified several key properties of the omission responses. In particular, our results demonstrate that the omission responses depend on different parameters, including the repetition rate, brain state but are similar across species. According to our findings, omission-sensitive responses are already present under anesthesia and become even more pronounced under the awake condition in both number and strength. The omission responses are likely the earliest neuronal correlate underlying the salient perception of omitted stimuli in humans and can be considered to provide additional support for a hierarchical predictive coding framework (*1*, *37*, *39*, *42*, *43*).

Relation to previous studies

In humans, responses to omissions of tones are primarily observed at rather high presentation rates (*15*, *16*), corresponding to the presently used shortest SOA. To resolve these on the neuronal level, the high temporal resolution available in electrophysiology is highly suited. On the basis of single-unit recordings, our study demonstrates clear omission responses at the spiking level in the auditory system and thus identifies a potential neuronal correlate for those omission responses previously recorded using noninvasive techniques such as EEG/magnetoencephalography in humans (*9*, *16*, *25*, *44*–*49*).

Multiple studies have investigated mismatches between predictions and actual stimuli on the neuronal level using calcium imaging in different sensory cortices. While calcium imaging provides the possibility for highly parallel recordings, its temporal resolution limits the use of comparably fast SOAs in continuous sequences as in the present study. In the visual cortex V1 in the mouse, multiple studies reported responses to sequence violations

[e.g., (*50*–*52*)], as well as in the somatosensory system (*53*). In the auditory system, virtually no, if any, studies have directly looked for omission responses at the cellular level, or have not directly reported them (*7*, *8*, *13*, *34*, *54*, *55*). Two studies have reported potentially related results using calcium imaging: Li and colleagues (*56*) have reported neural responses at the end of a regular, slow train of repetitive stimuli as a persistent evoked response, which they termed echo responses (*56*, *57*). While those echo responses might also signal predictions, the much slower time scales (SOA: 2 to 4 s) suggest different underlying mechanisms. Possibly because of limitations imposed through the calcium dynamics, the studies did not find omission responses at fast rates. Given the shorter SOAs, we observe strong adaptation to the tones, while such adaptation appears to be absent in the longer SOAs for the echo responses, which suggests a difference in the contributing mechanisms. Other differences between omission and echo responses include latency and histological location: The latency of the present omission and stimulus responses was similar, which indicates that the omission responses are time-locked to the expected time of occurrence of the omitted stimuli. In contrast, the latency of the echo responses is significantly longer than that of the stimulus responses (237 versus 83 ms) (*57*). Omission responses are found in subcortical neurons, at the IC level, while the echo responses seem to only emerge at the cortical level (*56*). Moreover, these authors (*56*) also discuss very elegantly how their echo responses differ from the classical omissions recorded under the oddball paradigm as we do here. Li and colleagues (*56*) relate these responses to fit the time scales of motor responses. This is a key aspect of their work as their results strongly support that the neuronal circuits of the AC are critical for coding predictive information and transforming it into anticipatory motor behavior. There is also other work that is also similar in some ways to the echo responses but recorded in the IC, the so-called "long-lasting sound-evoked afterdischarge" responses or LSA neurons (*58*). These authors argue that, because LSA produces long-lasting firing in the absence of sound, it may be relevant to temporary or chronic tinnitus or to some other aftereffect of long-duration sound. While it thus appears that omission, LSA responses, and echo responses rely on different underlying mechanisms, the use of different stimulation paradigms and recording procedures complicates a conclusive comparison.

Earlier theoretical investigations using neural modeling had already suggested the existence of omission responses (*20*, *59*). Omission responses were here created by the difference between the activity of neurons encoding the prediction of the next stimulus and the actual input (see the "Relation to predictive coding theory" section for more details).

Relevance of the current results

We have recorded robust omission responses in the auditory pathway of anesthetized rats and anesthetized and awake mice using single- and multiunit recordings. These statistically significant responses of single neurons evoked by omitted tones had the largest proportion (~36%) observed in the awake AC and the lowest at the urethane-anesthetized AC of rats (~20%) and mice (~22%). The difference in the detected omission responses appears to be determined most strongly by brain state, because we did not find a significant difference between the omission response size in the AC between the anesthetized rat and mouse. The fact that we found omission responses also in anesthetized preparations suggests that omission detection and thus predictive coding are already partially available under the passive condition, without the need for specific attention (*8*, *23*). Furthermore, the proportion of omission responses was only substantially present at the shortest SOA of 125 ms, i.e., at relatively high presentation rates (up to 8 Hz). This time course suggests that if the sounds are close enough in time, then they form a perceptual unit and, hence, compatible with the temporal window of integration (*15*, *16*, *60*, *61*) that integrates neighboring sounds and/or omissions into a single percept.

While we could not find significant differences when the omission responses were preceded by a random number of reference stimuli (random), compared to a fixed number of reference stimuli (periodic), several studies have shown that expected omissions evoke a smaller response than unexpected omissions (*19*, *25*, *45*). It may be that the number of preceding repetitions (nine stimuli) in our periodic sequences is too large for producing an accurate expectation of when it should happen in our rodent models; if the animal loses track of how many repeated stimuli have happened, then these omissions would be perceived as events preceded by a random (albeit large) number of stimuli. This is supported by the rapid dynamics of adaptation or the responses to the standard stimulus following the omission, which return to baseline in just one to two stimuli (Fig. 7). Related to this, we only find a correlation between the number of preceding stimuli and the omission response under the anesthetized condition, while it may have already reached a plateau in the awake case. This finding relates to the previous work by Dürschmid *et al.* (*62*), which demonstrated that transitional probabilities are different in AC and prefrontal cortex by increasing the number of standards before a deviant occurrence. They observed that this increases the expectation of prediction errors in the prefrontal cortex, while this was not the case for the AC (*62*). This is in accordance with our data related to the number of preceding standard responses before an omission that did not show an enhancement but a sustained response. This is important because omission-selective responses have been reported in humans (*19*, *27*, *44*, *63*, *64*), suggesting the preactivation of neural circuits needed to process the actual physical inputs.

Additional related work in humans has shown an interaction between arousal (in the form of attentional set and expectation) and mismatch responses. For example, an elegant study by Auksztulewicz and Friston (*65*) concluded that temporal attention and sensory expectation produced opposing effects on evoked response amplitude, when orthogonally manipulated in an auditory mismatch paradigm. MMN was enhanced by attention, speaking against its supposedly preattentive nature. The distinction between expectation and attention may be useful when interpreting our results in the awake mice. In other words, there is a difference between expecting something and attending to a sensory stream, and these can have opposite effects on the amplitude of mismatch responses (and thus, presumably, omission-related responses).

Methodological considerations

An important strength in our study is that we have used two animal species and two different recording preparations in two different laboratory setups. This approach allowed us to distinguish the effect of species and brain state on the omission responses and demonstrate that the results under anesthesia do not differ significantly between mice and rats, mimicking previous results (*66*–*70*). In contrast, the frequency of omission-sensitive cells and the magnitude of

the omission responses were found to be larger in awake mice than under anesthesia. This would be in line with the differences in the level of response for humans in awake compared to unresponsive wakefulness state [see, e.g., (*67*)]. Furthermore, this is also consistent with our previous work comparing rat, mouse (*8*, *71*, *72*), and others that show a similar structural and functional organization of these rodents' auditory system [e.g., (*73*–*75*)], speaking in favor of the existence of genuine omission responses across species that can be modulated by arousal state.

It is unlikely that the omission responses we observed are not genuine responses or simply the reflection of rebound or entrainment effects as discussed elsewhere in the context of adaptation models (*17*, *76*) and our own control data shown in fig. S5. If these omission responses were just long latency activity evoked by the previous stimulus, then such activity would remain when probing the neurons with longer SOA sequences, but that is not the case in our data (see fig. S5). In addition, such an adaptation model would not account for omissions evoking a larger response than the tone they replaced as occurring in many of our responses; if anything, the effect would be opposite. Moreover, there are also models that support the predictive framework for omission responses. The modeling study by Wacongne *et al.* (*19*, *20*) demonstrated that omission responses were larger than stimulus responses in blocks containing quintuplets of tones where the last one was replaced by an omitted tone, whereas the adaptation model would predict equal omission responses in both instances. Moreover, entrainment should be stronger for periodic sensory stimuli (*77*).

Although there is no question that omission responses occur in AC, a relevant weakness in our study is that AC responses are biased toward A1 (lemniscal field) in the awake mouse and toward the nonlemniscal fields in the anesthetized rat, making it difficult to conclude if the differences in the response magnitude between the two preparations are related to the arousal state or the field location of the recordings. Although the results are in line with the hierarchical organization of prediction error that we have seen in our previous studies (*8*), future studies should clarify this confound.

We found a relatively small percentage (16.7%) of omission neurons in the IC of the anesthetized rat, at least compared to the amount of omission neurons in the anesthetized rats (19.5%) and mice (21.7%), as well as awake mice AC (35.6%). In the split data analysis, the IC responses are revealed to be less robust or statistical deviations. While the omission responses in the IC are thus not as robust as in the AC, the fact that the IC recordings were underpowered and were only conducted in the anesthetized state preclude a conclusion on the existence of omission-sensitive responses in the IC. For example, a recent study showed that a small proportion of IC neurons were pattern sensitive (*78*) and that a sparse set (~5%) of neurons in AC showed a high-rate prolonged burst firing responses to trained sounds (*79*). Further studies in the IC under the awake state with greater neuron numbers are required to resolve this question.

Relation to predictive coding theory

As in other sensory systems, where omission responses have been best explained by a deviation between expected and actual visual stimulus (*50*), our results are consistent with a predictive coding framework, in which sensory input is compared to an internal model of the environment to detect deviations from expectations. Because bottom-up inputs cannot account for omission responses, our results are consistent with the hypothesis that prediction is a hierarchical process encompassing subcortical and cortical neuronal circuitries and can be observed in two species and two brain states. Together, these findings are in agreement with two recent studies that have combined 9.4-T functional magnetic resonance imaging and high-density electrocorticographic recordings with a local-global auditory sequence paradigm to assess the hierarchical depth of auditory sequence processing in the marmoset brain (*80*, *81*). These authors demonstrate that the neural responses to omissions cannot be explained by any modulation of feedforward propagation and should contain specific information of upcoming predictive information (*80*, *82*). Hence, omission responses thus allow the study of top-down prediction signals decoupled from bottom-up input signals, i.e., without sensory input. Such a perspective supports the notion of an endogenous neural activity that could reflect the generation of predictions (*83*, *84*).

An important issue to be considered is whether responses encoding predictions can be disentangled from responses encoding prediction errors. According to predictive coding, omission responses can provide rather clear access to the representation of the prediction; as in this case, the prediction error is a, in the forward path inverted, copy of the prediction (*26*, *85*). Because the omission responses that we detected are elevations in firing rate, they likely provide access to the neural representation of prediction in the AC (*64*, *81*, *86*). Another distinction between prediction error and prediction responses may be feasible in time-frequency measures (*87*, *88*). Thus, positive omission responses are likely related to predictions (*10*, *21*) and within predictive coding theory represented by interneuron-mediated modulation of pyramidal output. Hence, they may share the neuronal and local circuitry of stimulus-specific adaptation that involves multiple neuron types (*35*, *89*, *90*), supporting feedforward and feedback inhibition and excitation of pyramidal output, which can detect deviations from regularity (*35*, *59*). Our data do not allow us to definitely distinguish whether we recorded from excitatory or inhibitory interneurons; we have observed omission responses in multiple AC layers that encompass different neuron types, suggesting that omission responses are generated and enhanced at the network level through a hierarchical process consistent with the predictive coding perspective (*1*, *37*–*39*, *43*, *84*, *91*). Canonical microcircuit formulations of predictive coding are quite consistent: They suggest that excitatory pyramidal cells encode prediction errors (*92*, *93*). Their activity is the difference between ascending stimulus information and the activity of interneurons. In this formulation, the interneurons represent the predictions, e.g., derived from regularities in the environment. The pyramidal cells are hypothesized to be located in superficial and granular layers, while the prediction carrying inhibitory neurons are hypothesized to be located in supragranular layers. However, the latter activity is also thought to be passed to infragranular pyramidal cells (*92*). This architecture makes it difficult to have a simple hypothesis of where omission-related responses should be found. This follows because they could be associated with predictions in deep pyramidal cells or the inhibitory interneurons in superficial layers. However, a more definitive interpretation would probably rest upon tracing studies or optogenetic characterization of the cells recorded. Thus, future studies are needed to separate pyramidal neurons from inhibitory interneurons to get a clearer picture of predictive coding in canonical microcircuits.

Another interesting, yet difficult, issue to resolve is how the different components described in the classical adaptation studies, i.e., prediction error and repetition suppression (*8*), relate to the deviant and omission responses. To address this issue, it would have been necessary to carry out additional control recordings using the cascade or many-standard sequence as in, e.g., (*8*, *23*, *35*, *94*). Unfortunately, these sequences are very time consuming and the current inclusion of other conditions (multiple SOAs, deviant) precluded the recording of these additional controls. This is definitely an interesting and open question but a limitation of the current study that should be explored in the future. In summary, the demonstration of omission responses in IC and AC, particularly in awake but also in anesthetized preparations, confirms that the auditory system does not require an external stimulus trigger to detect a deviation from expectations (*95*) and indicates that the auditory brain internally generates a prediction of future sensory input.

MATERIALS AND METHODS

Experimental procedures

Experiments were performed on 22 anesthetized adult female Long-Evans rats (9 rats were used for IC recordings and 13 rats for AC recordings) and 6 C57/B6 mice (3 awake and 3 under urethane anesthesia). The body weight ranged from 200 to 300 g in rats (9 to 17 weeks of age) and 25 to 35 g in mice (14 to 18 weeks of age). Each individual animal was used to record from a single auditory station, either IC or AC. Experimental procedures in anesthetized rats were carried out at the University of Salamanca, and all the experimental procedures and protocols were adjusted to the directives of the Directive of the European Communities (86/609/CEE, 2003/65/CE, and 2010/63/UE) and RD53/2013 Spanish Legislation for the use and care of animals. All the details of the study were approved by the Bioethics Committee of the University of Salamanca (USAL-ID-195 and USAL-ID-574). Experiments in awake mice were performed at the Central Dierenlaboratorium at the Radboud University Medical Center. The experimental procedures and protocols were approved by the Dutch central commission for animal research (Centrale Commissie Dierproeven) and implemented according to approved work protocols from the local animal welfare body (project number 2017-0041).

Experimental procedures in anesthetized rats

The experiments were carried out inside a chamber with acoustic insulation and electrical protection. Sound stimuli were generated using the RZ6 Multi I/O processor [Tucker-Davis Technologies (TDT)]. Sounds were presented monaurally (right ear) through a closed system using a custom-made earphone (1 to 45 kHz) coupled to a custom-made cone, as a substitute for traditional ear bars. Thus, sounds were presented through the speaker under a closed-field condition to the ear contralateral to the left IC or AC.

The software was programmed with OpenEx Suite (TDT) and MATLAB. The sound system response was flattened with an on-site calibrated finite impulse response system using a one-fourth-inch condenser microphone (model 4136, Brüel & Kjaer), a conditioning amplifier (Nexus, Brüel & Kjaer), and a dynamic signal analyzer (Photon+, Brüel & Kjaer). The speaker output was adjusted to ensure a flat spectrum (±2 dB) between 0.5 and 44 kHz, and the second and third harmonic components in the signal were >40 dB below the level of the fundamental at the highest output level [~76 dB of sound pressure level (SPL)]. A single neuron was recorded at a time, using a self-made glass-coated tungsten electrode whose impedance ranged from 1.5 to 3 megohm at 1 kHz.

Analog signals were digitized with an RZ6 multi-I/O processor, Medusa RA16PA preamp, and ZC16 main stage (TDT) at 25 kHz of sample rate and amplified 251×. The neurophysiological signals for multi- or single-unit activity were band-pass filtered between 0.5 and 4.5 kHz.

Experimental procedures in anesthetized and awake mice

The experiments were carried out inside an acoustically insulated and electromagnetically shielded and grounded booth. Sound stimuli were generated and recorded using a multichannel data acquisition device (USB-6351, National Instruments) through a custom-written MATLAB GUI (Controller). Sounds were presented to both ears using a speaker (T250D, Fostex) placed in front and above the animal. The output of the speaker was calibrated to have a flat spectral profile over the range of 2 to 80 kHz within 5 dB using an inverse linear filter, estimated before the experiment using an ultrasonic microphone (CM16/CMPA, Avisoft Bioacoustics) corrected for its own frequency-dependent sensitivity curve.

Surgical procedures in anesthetized rats

The initial surgical procedures were the same for the two auditory areas to be recorded (IC and AC). Electrophysiological procedures differed only in craniotomy location and recording electrode placement for each station.

Anesthesia was induced and maintained with urethane [1.9 g/kg, intraperitoneally (ip)] with supplementary doses (~0.5 g/kg, ip) administered as necessary. These replenishments were given to ensure a deep and stable anesthetic level whenever corneal or pedal retraction reflexes appeared. Urethane maintains a balanced neuronal activity better than other anesthetic agents that have a slight effect on inhibitory and excitatory synapses and that is why it was the selected anesthesia method (*96*).

At the beginning of surgery, both dexamethasone (0.25 mg/kg) and atropine (0.1 mg/kg) were administered to reduce cerebral edema and bronchial secretions, respectively. Lidocaine was also injected around the pinna tissue to achieve a higher anesthetic level in these areas (*8*). In addition, an isotonic glucosaline solution [5 to 10 ml every 6 to 8 hours, subcutaneously (sc)] was periodically administered to avoid dehydration. During all the experimental procedures, the animals were artificially ventilated, controlling the CO_2 levels, and the temperature was monitored with a rectal probe (36° to 38°C) and maintained with a heating blanket (Cibertec) placed under the animal.

Once the animal reached a surgical state of anesthesia, the ears were prepared by removing the cartilage to obtain a greater exposure of the ear canal. The trachea was cannulated to maintain ventilation artificially, and corneal and pedal withdrawal reflexes were constantly monitored to ensure that we maintained a deep anesthetic level during surgery and as uniform as possible throughout the recording procedure.

Once the animal was prepared, it was placed on the stereotactic frame; the upper jaw was attached to a bite bar and the restraint was carried out using ear bars. At this time, the speaker was also placed on the right ear of the animal, while the left ear canal was covered with plasticine.

Surgical procedures for IC (anesthetized rats)

For IC recordings, a craniotomy was performed on the left parietal bone to expose the cerebral cortex overlying the left IC. The dura was removed and the surrounding tissue was covered with cotton balls soaked in 0.9% saline solution to maintain hydration of the area.

Surgical procedures for AC (anesthetized rats)

For AC recordings, the skin and temporal muscles were removed from the left side of the skull and a 6-mm by 5-mm craniotomy was performed on the left temporal bone to expose the entire AC. The dura was removed and the cisterna magna was drained to prevent brain herniation. The exposed cortex area and surrounding tissue were covered with a transparent layer of agar to prevent desiccation and, thus, stabilize the recordings.

Surgical procedures for AC (awake and anesthetized mice)

Mice were implanted with a headpost for head fixation at the ages of 8 to 12 weeks. In the second surgery, performed when animals were 12 to 16 weeks old, mice were implanted with a silicon NeuroNexus neural probe aiming at the left primary AC, field A1, based on stereotaxic coordinates (3.2 mm post-bregma, 5.9 mm lateral from the midline) measured on the skull, estimated from (*97*), and confirmed preimplantation via intrinsic optical imaging of noise burst sequences (0.2-s long, 0.1 s interstimulus interval, 70 dB of SPL, 10 sounds per trial, 30 trials). A craniotomy (~1 mm by 2 mm) was opened using a microdrill centered on the part of AC that showed the strongest response in the intrinsic imaging. In the awake mice, the implant was chronic, mounted on a custom-designed drive (variant of the EDDS drive, Microprobes for Life Science), allowing the electrode array to be repositioned. The surgery was performed under general isoflurane anesthesia (1.5 to 2% dosage; E-Z Anesthesia, E-Z Systems Corporation). From 24 hours before to 48 hours after the surgery, the animal received an analgesic dissolved in water (1 ml/liter; carprofen (Rimadyl cattle), Zoetis], supplemented by another dose of carprofen at the start of the surgery (5 mg/kg, sc). In the anesthetized mice, the electrode array was inserted acutely for the period of the recordings under urethane anesthesia using one initial dose (1.7 g/kg, ip) and one to two supplementary doses (0.2 g/kg, ip). In addition, dexamethasone (0.2 mg/kg, sc) was given under both conditions after induction of anesthesia to reduce local bulging of the brain, and a ground screw was implanted over the right frontal cortex.

Electrophysiological recording procedures

Auditory brainstem response recording in anesthetized rats

Once the animal was under anesthesia, before starting the surgery and therefore the recording sessions, the auditory brainstem responses were recorded using subcutaneous electrodes to ensure that the animal had normal hearing, using the RZ6 Multi I/O processor (TDT) as hardware and BioSig software (TDT). The auditory brainstem response stimuli were generated following standard procedures (0.1ms clicks presented at a rate of 21 Hz, applied monaurally to the right ear in 10 dB of upward steps between 10 and 90 dB of SPL using a closed-field speaker).

Procedures for electrophysiological recording in IC (anesthetized rats)

For measurements in the IC, an electrode was placed orthogonal to the surface of the brain (forming an angle of 20° with the horizontal plane, oriented caudally), advanced between 7500 and 10,000 μm from lambda to bregma and 500 and 3000 μm to the left ear, and then lowered into the brain between 4400 and 5600 μm using a piezoelectric micromanipulator (Sensapex) until we observed a strong spike activity synchronized with the search stimulus train.

Procedures for electrophysiological recording in AC (anesthetized rats)

Once the AC was exposed and the tissue was stabilized, an enlarged image of the exposed surface was taken (×25). The image included a pair of landmarks previously marked before the craniotomy, on the dorsal border of the temporal bone, indicating the absolute scale and position of the image relative to bregma. This image was displayed on a computer screen, and a grid was overlaid on it that would serve as a guide so we would be able to mark the recording electrode placement for each recording. The snapshot was taken with a single lens digital reflex camera (D5100, Nikon) coupled to the surgical microscope (Zeiss) through a lens adapter (TTI Medical) (*7*).

For AC measurements, we placed the electrode in contact with the AC and as perpendicular as possible to its surface. After this, we advanced it between 0 and 2000 μm in depth. The recording tracks were spaced 250 to 500 μm and placed through the cortical regions of interest, while blood vessels were avoided. The vascular pattern was used as a local reference to mark the position on the image where the tract was made, considering that this map varies between animals. At the end of the experiment, the limits and the relative position of the auditory fields were identified according to the pure-tone frequency response topographies in rats (*7*). We estimated the depth of each neuron from the reading of the micromanipulator relative to the brain surface (Fig. 8A). We used the depths of the layers in the rat AC as stated by Pérez-González *et al.* (*35*) (i.e., the granular layer would extend between 457 and 614 μm).

The characteristic frequency of each recording track was calculated as the average characteristic frequency of all neurons recorded on that track, including a rapid multiunit activity frequency response area recording performed between 400 and 550 μm in depth, corresponding to layers IIIb to IV. The reversals of the characteristic frequency progression defined the boundaries between the cortical fields (*98*), so that most recordings could be assigned to one specific field: primary or secondary and their corresponding subdivisions: AAF, VAF, A1, PAF, and SRAF.

Procedures for electrophysiological recording in AC (awake mice)

For the time of the recording, the animal was placed on a platform located in the middle of a booth and head-fixated using an implanted headpost. All recordings were performed using NeuroNexus silicon probes with 64 channels. The recording sites were distributed differently per probe; in particular, we used two 4x16 (A4x16-Poly2-5mm-23s-200-177 and A4x16-2.5mm-tet/lin-300/125-333-121/177-PC) configurations. Data were digitized using a combination of a 64-channel (Intan Technologies) headstage connected to an Open Ephys recording system (Open Ephys, Cambridge, USA). Data were collected at a sampling rate of 30 kS/s, band-pass filtered between 0.3 and 6 kHz, and spike-sorted to get multi- and single-unit responses using the openly available function autoSortC from the Controller package. The sorting used automatic criteria for cluster-cutting rather than human decisions, which are prone to be variable from day to day. Sorting was performed separately for each prong. The average number of cells/electrode in a single

session was 0.71 after spike-sorting, which is a typical yield, e.g., in comparison to other recording techniques (0.625 cells per electrode) (*99*). We estimated the depth of each cell from the depth of the array relative to the brain surface and the position of the recording sites in each array configuration (Fig. 8). The depths of the layers were estimated from a coronal section of the mouse AC in the Allen Brain Atlas (*100*) (i.e., the granular layer would extend between 355 and 477 μm).

Location of cells and recording of the frequency response area (anesthetized rat)

The sounds used to search for neuronal activity were trains of noise or pure tones (1 to 4 stimuli/s). These stimuli had a short duration (30 ms) to avoid a strong adaptation. Sound parameters such as frequency, intensity, presentation rate, or type of sound such as white noise, narrow band noise, or pure tones were manually varied as necessary to facilitate mismatch.

For each neuron recorded, the frequency response area was calculated, which is the response magnitude map for each pair of frequency/intensity data. This was calculated in the first place to ensure that the frequencies and intensities used were contained in the response range. To obtain this frequency response area, a sequence of tones was presented at a rate of 4 Hz, randomly varying the frequency and intensity of the tones presented (three to five repetitions of each tone).

For the AC recordings, the coordinates of the neurons over the AC extension were measured from the micromanipulator as the position of the recording electrode in reference to bregma. For the IC recordings, at the end of the recording session, a 5-μA current was driven for 5 s through the recording electrode to produce an electrolytic lesion. Animals were euthanized with a lethal dose of pentobarbital, and the head was removed and immersed in a mixture of 1% paraformaldehyde and 1% glutaraldehyde in 1 M phosphate-buffered saline. After fixation, tissue was cryoprotected in 30% sucrose and sectioned in a freezing microtome to obtain 40-μm-thick coronal sections. The sections were stained using 0.1% cresyl violet to facilitate identification of cytoarchitectural boundaries.

Online viewing

For the anesthetized experiments, we visualized the electrophysiological recordings online using custom-written software with MATLAB (MathWorks) and OpenEx Suite (TDT). Multiple-unit activity was automatically extracted by manually setting a unilateral action potential threshold above the background noise as an accurate estimate of neuronal population dynamics (*101*). Once a neuron was isolated and confirmed to be stable, the stimulation protocol described in the next section was applied. For the awake experiments, the activity was monitored online using the Open Ephys GUI, and stimuli were presented if single-unit neural activity could be visually detected.

Stimulation parameters

The sounds used for stimulation were sinusoidal tones of 75-ms duration, including up and down ramps of 5 ms, at a frequency and intensity within the response area of the neuron. In the single-electrode recordings in the rat, the frequency-intensity combination could be chosen specifically for the single neuron recorded at a time. In the many-electrode recordings in the mouse, we chose a set of frequencies that made a good match with the frequency response areas of the currently recorded cells. We used a fixed set of three intensities in the mouse ([50,60,70] dB of SPL) that were intense enough to activate all recorded neurons. These sounds were presented in an oddball sequence of 400 tones long. The oddball sequence consisted of a repeating tone (90% standard probability) that was occasionally omitted (10% deviant probability).

The omission of the tone was presented in two different ways within the oddball sequence: periodically or randomly, always with the same probability of appearance. A minimum of three standard tones were presented before each deviant. These sequences were presented with different SOAs (125, 250, and 500 ms) to control for confusion between actual responses to omissions and responses to previous standard stimuli. To double-check that no sound was played during omissions, we recorded the output of the speaker while playing the stimulation sequence to check that there was no acoustic signal during the omissions (fig. S1).

In a second set of recordings, we compared deviant tones with omission responses in the AC of anesthetized rats and awake mice (Fig. 6). For this purpose, identical sequences were used with either deviant tones or omissions occurring at the same positions in the sequence. In the single-electrode recordings in the rat, the standard and deviant frequencies were chosen to lie symmetrically around the characteristic frequency at the same intensity to elicit similar response rates (Fig. 6A). The paradigm was run with either of the two stimuli as standard and deviant. In the multielectrode recordings in the mouse, we chose a pair of frequencies that provided the best match to the currently recorded cells and also ran the paradigm with both frequencies for standard and deviant. All subsequent analyses for omissions and deviants were identical. Comparisons were then performed on the set of omission-sensitive neurons.

The output of the system was also recorded using a one-fourth-inch condenser microphone (model 4136, Brüel & Kjaer) to ensure the absence of any sound or noise during omissions (fig. S1). The spectrogram in fig. S1A shows a portion of the presented periodic omission sequence, reflecting the intensity of the sounds that the system reproduces. The power spectrum shown in fig. S1B allows comparison between the signal produced during a real stimulus (blue) and the omitted signal (red) and confirms that no sound was reproduced during the omission.

Data and statistical analysis

After the single- and multiunit response times were established, we selected the cells that elicited responses for omissions. We did that by comparing firing rates during omitted tones to the pre-stimulus firing rates. For this purpose, comparison windows had to be defined. The pre-stimulus/stimulus windows were defined individually for each SOA. These windows were chosen after visual inspection of the responses, aiming to include the bulk of the evoked responses while leaving enough time to calculate the pre-stimulus activity for the next trial. Because of the long AC responses, for the 125 SOA recordings, there is some overlap between the pre-stimulus and stimulus windows. The pre-stimulus window start was defined as 25, 75, and 195 ms before the stimulus onset for 125, 250, and 500 ms of SOA, respectively. All pre-stimulus windows ended 5 ms after the start of the stimulus, because the evoked response latency was always longer great than 5 ms. This time also marks the start of the "stimulus window." Stimulus windows ended at 120, 150, and 225 ms for 125, 250, and 500 ms

of SOA, respectively. Note that stimulus here refers to both tone and omission. These values are summarized in Table 3.

Firing rates were computed in all of the predefined windows and used in subsequent analyses to compare the responses under the tested conditions. PSTHs (10-ms bins; Fig. 2 and fig. S5) were aligned to show the average response around the omission. Peak latencies were calculated for each tone or omission as the time (relative to stimulus onset) of the maximum value in the stimulus PSTH (1-ms bins).

Omission responses were identified as an elevated firing rate during the omitted tones. Specifically, responses during the omission window were considered significant if their mean firing rate was significantly larger than the mean firing rate of the cell's activity, immediately preceding the omission window.

Using these time windows, we collected for each omission the firing rates of preomission activity and the firing rates of omission activity. To avoid a positive bias due to double dipping, we used split data analysis (*32*), i.e., only every other omission was used for statistical testing, while the complementary set was used for all subsequent analyses. These sets are referred to as "statistics set" and "analysis set." The starting point, the first or second omission, for the division into the two sets was randomized independently between cells, i.e., either using the omissions at positions [1, 3, 5, ...] or [2, 4, 6,...] for the statistics set and, correspondingly, the complement for the analysis set. In the statistics set, the preomission activity was compared against the periomission activity over the length of the stimulus window (see above) using a single-sided paired Wilcoxon signed-rank test. A neuron was termed an "omission-sensitive neuron" if the P value was <0.05. False positives in this classification will not translate to elevated omission responses, based on the split data analysis, where only systematic differences, present in both splits of the data, are retained in the plotting. The significance on the population level is then subsequently tested on the part of the data not used for statistical testing (see Fig. 3).

The iOmi used to quantify the comparison between sound- and omission-evoked firing rate (Fig. 4A) was defined as: iOmi = (Omi FR − Stim FR)/(Omi FR + Stim FR). The firing rate for stimuli was averaged from all stimulus presentations.

The statistical analysis on the population level was performed using ANOVA (Kruskal-Wallis analysis for one-way comparisons) followed by pairwise comparisons between individual conditions using Wilcoxon signed-rank test with Bonferroni correction for the number of tests performed. Rates were transformed to approximately normal distributions by taking their logarithm, given that neural responses are distributed exponentially particularly at low rates. For differences between firing rates, e.g., stimulus versus omissions, we computed the logarithm of the difference in rates, before applying ANOVA.

For testing whether the percentage of omission-sensitive neurons in each layer was as expected if these neurons were randomly distributed across layers, we sampled the same number of omission-sensitive neurons according to the empirical distributions across layer groups (i.e. granular, infragranular, and supragranular) using bootstrapping (300,000 samples) and then compared the actual distribution of omission-sensitive cells to the bootstrapped densities. The P values represent their location in the distribution at the closest end of the density.

Table 3. Times of the analysis windows, relative to stimulus/omission onset.

SOA	Pre-stimulus window start	Pre-stimulus window stop/stimulus window start	Stimulus window stop
125	−25 ms	5 ms	120 ms
250	−75 ms	5 ms	150 ms
500	−195 ms	5 ms	225 ms

Supplementary Materials

This PDF file includes:
Figs. S1 to S5
Legend for data S1

Other Supplementary Material for this manuscript includes the following:
Data S1

View/request a protocol for this paper from *Bio-protocol*.

REFERENCES AND NOTES

1. K. Friston, A theory of cortical responses. *Phil. Trans. R. Soc. B* **360**, 815–836 (2005).
2. I. Winkler, Interpreting the mismatch negativity. *J. Psychophysiol.* **21**, 147–163 (2007).
3. M. I. Garrido, K. J. Friston, S. J. Kiebel, K. E. Stephan, T. Baldeweg, J. M. Kilner, The functional anatomy of the MMN: A DCM study of the roving paradigm. *Neuroimage* **42**, 936–944 (2008).
4. H. E. M. Den Ouden, K. J. Friston, N. D. Daw, A. R. McIntosh, K. E. Stephan, A dual role for prediction error in associative learning. *Cereb. Cortex* **19**, 1175–1185 (2009).
5. H. E. M. Den Ouden, P. Kok, F. P. de Lange, How prediction errors shape perception, attention, and motivation. *Front. Psychol.* **3**, 548 (2012).
6. G. Stefanics, P. Astikainen, I. Czigler, Visual mismatch negativity (vMMN): A prediction error signal in the visual modality. *Front. Hum. Neurosci.* **8**, 1074 (2015).
7. J. Nieto-Diego, M. S. Malmierca, Topographic distribution of stimulus-specific adaptation across auditory cortical fields in the anesthetized rat. *PLOS Biol.* **14**, e1002397 (2016).
8. G. G. Parras, J. Nieto-Diego, G. V. Carbajal, C. Valdés-Baizabal, C. Escera, M. S. Malmierca, Neurons along the auditory pathway exhibit a hierarchical organization of prediction error. *Nat. Commun.* **8**, 2148 (2017).
9. A. Bendixen, I. SanMiguel, E. Schröger, Early electrophysiological indicators for predictive processing in audition: A review. *Int. J. Psychophysiol.* **83**, 120–131 (2012).
10. G. V. Carbajal, M. S. Malmierca, The neuronal basis of predictive coding along the auditory pathway: From the subcortical roots to cortical deviance detection. *Trends Hear.* **22**, 233121651878482 (2018).
11. G. V Carbajal, M. S. Malmierca, Novelty processing in the auditory system: Detection, adaptation or expectation?, in *The Senses: A Comprehensive Reference*, B. Fritzsch, B. Gothe, Eds. (Elsevier, ed. 2, 2020), pp. 749–776.
12. A. Yuille, D. Kersten, Vision as Bayesian inference: Analysis by synthesis? *Trends Cogn. Sci.* **10**, 301–308 (2006).
13. F. M. Antunes, I. Nelken, E. Covey, M. S. Malmierca, Stimulus-specific adaptation in the auditory thalamus of the anesthetized rat. *PLOS ONE* **5**, e14071 (2010).
14. R. P. N. Rao, D. H. Ballard, Predictive coding in the visual cortex: A functional interpretation of some extra-classical receptive-field effects. *Nat. Neurosci.* **2**, 79–87 (1999).
15. M. Tervaniemi, J. Saarinen, P. Paavilainen, N. Danilova, R. Näätänen, Temporal integration of auditory information in sensory memory as reflected by the mismatch negativity. *Biol. Psychol.* **38**, 157–167 (1994).
16. H. Yabe, M. Tervaniemi, K. Reinikainen, R. Näätänen, Temporal window of integration revealed by MMN to sound omission. *Neuroreport* **8**, 1971–1974 (1997).
17. P. J. C. May, H. Tiitinen, Mismatch negativity (MMN), the deviance-elicited auditory deflection, explained. *Psychophysiology* **47**, 66–122 (2010).
18. J. Horváth, D. Müller, A. Weise, E. Schröger, Omission mismatch negativity builds up late. *Neuroreport* **21**, 537–541 (2010).

19. C. Wacongne, E. Labyt, V. Van Wassenhove, T. Bekinschtein, L. Naccache, S. Dehaene, Evidence for a hierarchy of predictions and prediction errors in human cortex. *Proc. Natl. Acad. Sci. U.S.A.* **108**, 20754–20759 (2011).
20. C. Wacongne, J. P. Changeux, S. Dehaene, A neuronal model of predictive coding accounting for the mismatch negativity. *J. Neurosci.* **32**, 3665–3678 (2012).
21. M. Heilbron, M. Chait, Great expectations: Is there evidence for predictive coding in auditory cortex? *Neuroscience* **389**, 54–73 (2018).
22. Y. M. Fonken, A. Mukerji, R. Jimenez, J. Lin, P. Brunner, G. Schalk, R. T. Knight, Unexpected sound omissions are signaled in human posterior superior temporal gyrus: An intracranial study. bioRxiv 733212 [Preprint]. 14 August 2019. https://doi.org/10.1101/733212.
23. L. Casado-Román, G. V. Carbajal, D. Pérez-González, M. S. Malmierca, Prediction error signaling explains neuronal mismatch responses in the medial prefrontal cortex. *PLOS Biol.* **18**, e3001019 (2020).
24. A. Bendixen, E. Schröger, I. Winkler, I heard that coming: Event-related potential evidence for stimulus-driven prediction in the auditory system. *J. Neurosci.* **29**, 8447–8451 (2009).
25. A. Todorovic, F. van Ede, E. Maris, F. P. de Lange, Prior expectation mediates neural adaptation to repeated sounds in the auditory cortex: An MEG study. *J. Neurosci.* **31**, 9118–9123 (2011).
26. E. Schröger, S. A. Kotz, I. SanMiguel, Bridging prediction and attention in current research on perception and action. *Brain Res.* **1626**, 1–13 (2015).
27. M. Cornella, A. Bendixen, S. Grimm, S. Leung, E. Schröger, C. Escera, Spatial auditory regularity encoding and prediction: Human middle-latency and long-latency auditory evoked potentials. *Brain Res.* **1626**, 21–30 (2015).
28. D. J. M. Kraemer, C. N. Macrae, A. E. Green, W. M. Kelley, Sound of silence activates auditory cortex. *Nature* **434**, 158 (2005).
29. M. S. Malmierca, Auditory system, in *The Rat Nervous System*, G. Paxinos, Ed. (Elsevier–Academic Press, ed. 4, 2015), pp. 865–946.
30. M. S. Malmierca, D. K. Ryugo, Descending connections of auditory cortex to the midbrain and brain stem. *Audit. Cortex*, 189–208 (2011).
31. R. Näätänen, A. W. K. Gaillard, S. Mäntysalo, Early selective-attention effect on evoked potential reinterpreted. *Acta Psychol. (Amst)* **42**, 313–329 (1978).
32. N. Kriegeskorte, W. K. Simmons, P. S. Bellgowan, C. I. Baker, Circular analysis in systems neuroscience: The dangers of double dipping. *Nat. Neurosci.* **12**, 535–540 (2009).
33. K. S. Button, Double-dipping revisited. *Nat. Neurosci.* **22**, 688–690 (2019).
34. M. S. Malmierca, S. Cristaudo, D. Pérez-González, E. Covey, Stimulus-specific adaptation in the inferior colliculus of the anesthetized rat. *J. Neurosci.* **29**, 5483–5493 (2009).
35. D. Pérez-González, G. G. Parras, C. J. Morado-Díaz, C. Aedo-Sánchez, G. V. Carbajal, M. S. Malmierca, Deviance detection in physiologically identified cell types in the rat auditory cortex. *Hear. Res.* **399**, 107997 (2021).
36. D. B. Polley, H. L. Read, D. A. Storace, M. M. Merzenich, Multiparametric auditory receptive field organization across five cortical fields in the albino rat. *J. Neurophysiol.* **97**, 3621–3638 (2007).
37. M. I. Garrido, J. M. Kilner, K. E. Stephan, K. J. Friston, The mismatch negativity: A review of underlying mechanisms. *Clin. Neurophysiol.* **120**, 453–463 (2009).
38. Z. C. Chao, K. Takaura, L. Wang, N. Fujii, S. Dehaene, Large-scale cortical networks for hierarchical prediction and prediction error in the primate brain. *Neuron* **100**, 1252–1266.e3 (2018).
39. K. Friston, S. Kiebel, Cortical circuits for perceptual inference. *Neural Netw.* **22**, 1093–1104 (2009).
40. F. P. de Lange, M. Heilbron, P. Kok, How do expectations shape perception? *Trends Cogn. Sci.* **22**, 764–779 (2018).
41. H. C. Barron, R. Auksztulewicz, K. Friston, Prediction and memory: A predictive coding account. *Prog. Neurobiol.* **192**, 101821 (2020).
42. K. Friston, Hierarchical models in the brain. *PLOS Comput. Biol.* **4**, e1000211 (2008).
43. F. Lieder, J. Daunizeau, M. I. Garrido, K. J. Friston, K. E. Stephan, Modelling trial-by-trial changes in the mismatch negativity. *PLOS Comput. Biol.* **9**, e1002911 (2013).
44. T. Raij, L. McEvoy, J. P. Mäkelä, R. Hari, Human auditory cortex is activated by omissions of auditory stimuli. *Brain Res.* **745**, 134–143 (1997).
45. S. Chennu, V. Noreika, D. Gueorguiev, Y. Shtyrov, T. A. Bekinschtein, R. Henson, Silent expectations: Dynamic causal modeling of cortical prediction and attention to sounds that weren't. *J. Neurosci.* **36**, 8305–8316 (2016).
46. T. T. Dercksen, A. Widmann, E. Schröger, N. Wetzel, Omission related brain responses reflect specific and unspecific action-effect couplings. *Neuroimage* **215**, 116840 (2020).
47. T. T. Dercksen, A. Widmann, F. Scharf, N. Wetzel, Sound omission related brain responses in children. *Dev. Cogn. Neurosci.* **53**, 101045 (2022).
48. D. A. Prete, D. Heikoop, J. E. McGillivray, J. P. Reilly, L. J. Trainor, The sound of silence: Predictive error responses to unexpected sound omission in adults. *Eur. J. Neurosci.* **55**, 1972–1985 (2022).
49. S.-L. Joutsiniemi, R. Hari, Omissions of auditory stimuli may activate frontal cortex. *Eur. J. Neurosci.* **1**, 524–528 (1989).
50. A. Fiser, D. Mahringer, H. K. Oyibo, A. V. Petersen, M. Leinweber, G. B. Keller, Experience-dependent spatial expectations in mouse visual cortex. *Nat. Neurosci.* **19**, 1658–1664 (2016).
51. G. B. Keller, T. Bonhoeffer, M. Hübener, Sensorimotor mismatch signals in primary visual cortex of the behaving mouse. *Neuron* **74**, 809–815 (2012).
52. A. Pak, S. T. Kissinger, A. A. Chubykin, Impaired adaptation and laminar processing of the oddball paradigm in the primary visual cortex of Fmr1 KO mouse. *Front. Cell. Neurosci.* **15**, 668230 (2021).
53. H. Mohan, Y. Gallero-Salas, S. Carta, J. Sacramento, B. Laurenczy, L. T. Sumanovski, C. P. J. De Kock, F. Helmchen, S. Sachidhanandam, Sensory representation of an auditory cued tactile stimulus in the posterior parietal cortex of the mouse. *Sci. Rep.* **8**, 7739 (2018).
54. N. Ulanovsky, L. Las, I. Nelken, Processing of low-probability sounds by cortical neurons. *Nat. Neurosci.* **6**, 391–398 (2003).
55. B. J. Farley, M. C. Quirk, J. J. Doherty, E. P. Christian, Stimulus-specific adaptation in auditory cortex is an NMDA-independent process distinct from the sensory novelty encoded by the mismatch negativity. *J. Neurosci.* **30**, 16475–16484 (2010).
56. J. Li, X. Liao, J. Zhang, M. Wang, N. Yang, J. Zhang, G. Lv, H. Li, J. Lu, R. Ding, X. Li, Y. Guang, Z. Yang, H. Qin, W. Jin, K. Zhang, C. He, H. Jia, S. Zeng, Z. Hu, I. Nelken, X. Chen, Primary auditory cortex is required for anticipatory motor response. *Cereb. Cortex* **27**, 3254–3271 (2017).
57. M. Wang, R. Li, J. Li, J. Zhang, X. Chen, S. Zeng, X. Liao, Frequency selectivity of echo responses in the mouse primary auditory cortex. *Sci. Rep.* **8**, 49 (2018).
58. M. Ono, D. C. Bishop, D. L. Oliver, Long-lasting sound-evoked afterdischarge in the auditory midbrain. *Sci. Rep.* **6**, 20757 (2016).
59. V. S. C. Chien, B. Maess, T. R. Knösche, A generic deviance detection principle for cortical On/Off responses, omission response, and mismatch negativity. *Biol. Cybern.* **113**, 475–494 (2019).
60. H. Yabe, M. Tervaniemi, J. Sinkkonen, M. Huotilainen, R. J. Ilmoniemi, R. Näätänen, Temporal window of integration of auditory information in the human brain. *Psychophysiology* **35**, 615–619 (1998).
61. Y. Mori, H. Hoshino, Y. Osakabe, T. Wada, K. Kanno, T. Shiga, S. Itagaki, I. Miura, H. Yabe, Omission mismatch negativity of speech sounds reveals a functionally impaired temporal window of integration in schizophrenia. *Clin. Neurophysiol.* **132**, 1144–1150 (2021).
62. S. Dürschmid, E. Edwards, C. Reichert, C. Dewar, H. Hinrichs, H. J. Heinze, H. E. Kirsch, S. S. Dalal, L. Y. Deouell, R. T. Knight, Hierarchy of prediction errors for auditory events in human temporal and frontal cortex. *Proc. Natl. Acad. Sci. U.S.A.* **113**, 6755–6760 (2016).
63. H. C. Hughes, T. M. Darcey, H. I. Barkan, P. D. Williamson, D. W. Roberts, C. H. Aslin, Responses of human auditory association cortex to the omission of an expected acoustic event. *Neuroimage* **13**, 1073–1089 (2001).
64. I. SanMiguel, A. Widmann, A. Bendixen, N. Trujillo-Barreto, E. Schröger, Hearing silences: Human auditory processing relies on preactivation of sound-specific brain activity patterns. *J. Neurosci.* **33**, 8633–8639 (2013).
65. R. Auksztulewicz, K. Friston, Attentional enhancement of auditory mismatch responses: A DCM/MEG study. *Cereb. Cortex* **25**, 4273–4283 (2015).
66. T. A. Bekinschtein, S. Dehaene, B. Rohaut, F. Tadel, L. Cohen, L. Naccache, Neural signature of the conscious processing of auditory regularities. *Proc. Natl. Acad. Sci. U.S.A.* **106**, 1672–1677 (2009).
67. U. Górska, A. Rupp, T. Celikel, B. Englitz, Assessing the state of consciousness for individual patients using complex, statistical stimuli. *NeuroImage. Clin.* **29**, 102471 (2021).
68. K. V. Nourski, M. Steinschneider, A. E. Rhone, H. Kawasaki, M. A. Howard, M. I. Banks, Auditory predictive coding across awareness states under anesthesia: An intracranial electrophysiology study. *J. Neurosci.* **38**, 8441–8452 (2018).
69. K. V. Nourski, M. Steinschneider, A. E. Rhone, B. M. Krause, H. Kawasaki, M. I. Banks, Cortical responses to auditory novelty across task conditions: An intracranial electrophysiology study. *Hear. Res.* **399**, 107911 (2021).
70. C. A. Smout, M. F. Tang, M. I. Garrido, J. B. Mattingley, Attention promotes the neural encoding of prediction errors. *PLOS Biol.* **17**, e2006812 (2019).
71. D. Duque, M. S. Malmierca, Stimulus-specific adaptation in the inferior colliculus of the mouse: Anesthesia and spontaneous activity effects. *Brain Struct. Funct.* **220**, 3385–3398 (2015).
72. Y. A. Ayala, D. Pérez-González, M. S. Malmierca, Stimulus-specific adaptation in the inferior colliculus: The role of excitatory, inhibitory and modulatory inputs. *Biol. Psychol.* **116**, 10–22 (2016).
73. M. S. Malmierca, D. K. Ryugo, Auditory system, in *The Mouse Nervous System* (Elsevier, 2012), pp. 607–645.

74. D. Choy Buentello, D. C. Bishop, D. L. Oliver, Differential distribution of GABA and glycine terminals in the inferior colliculus of rat and mouse. *J. Comp. Neurol.* **523**, 2683–2697 (2015).
75. H. Foley, M. Matlin, The auditory system, in *Sensation and Perception* (Psychology Press, 2015), pp. 258–284.
76. P. J. C. May, H. Tiitinen, Auditory scene analysis and sensory memory: The role of the auditory N100m. *Neurol. Clin. Neurophysiol.* **2004**, 19 (2004).
77. L. Gao, X. Meng, C. Ye, H. Zhang, C. Liu, Y. Dan, M. M. Poo, J. He, X. Zhang, Entrainment of slow oscillations of auditory thalamic neurons by repetitive sound stimuli. *J. Neurosci.* **29**, 6013–6021 (2009).
78. M. S. Malmierca, G. V Carbajal, C. Escera, Deviance detection and encoding acoustic regularity in the auditory midbrain, in *The Oxford Handbook of the Auditory Brainstem*, K. Kandler, Ed. (Oxford Univ. Press, 2019), pp. 706–740.
79. M. Wang, X. Liao, R. Li, S. Liang, R. Ding, J. Li, J. Zhang, W. He, K. Liu, J. Pan, Z. Zhao, T. Li, K. Zhang, X. Li, J. Lyu, Z. Zhou, Z. Varga, Y. Mi, Y. Zhou, J. Yan, S. Zeng, J. K. Liu, A. Konnerth, I. Nelken, H. Jia, X. Chen, Single-neuron representation of learned complex sounds in the auditory cortex. *Nat. Commun.* **11**, 4361 (2020).
80. Y. Jiang, M. Komatsu, Y. Chen, R. Xie, K. Zhang, Y. Xia, P. Gui, Z. Liang, L. Wang, Constructing the hierarchy of predictive auditory sequences in the marmoset brain. *eLife* **11**, e74653 (2022).
81. Y. Suda, M. Tada, T. Matsuo, K. Kawasaki, T. Saigusa, M. Ishida, T. Mitsui, H. Kumano, K. Kirihara, T. Suzuki, K. Matsumoto, I. Hasegawa, K. Kasai, T. Uka, Prediction-related frontal-temporal network for omission mismatch activity in the macaque monkey. *Front. Psych.* **13**, 557954 (2022).
82. G. Demarchi, G. Sanchez, N. Weisz, Automatic and feature-specific prediction-related neural activity in the human auditory system. *Nat. Commun.* **10**, 3440 (2019).
83. E. Schröger, A. Marzecová, I. Sanmiguel, Attention and prediction in human audition: A lesson from cognitive psychophysiology. *Eur. J. Neurosci.* **41**, 641–664 (2015).
84. A. Braga, M. Schönwiesner, Neural substrates and models of omission responses and predictive processes. *Front. Neural Circuits.* **16**, 799581 (2022).
85. B. Korka, A. Widmann, F. Waszak, Á. Darriba, E. Schröger, The auditory brain in action: Intention determines predictive processing in the auditory system—A review of current paradigms and findings. *Psychon. Bull. Rev.* **29**, 321–342 (2022).
86. I. SanMiguel, K. Saupe, E. Schröger, I know what is missing here: Electrophysiological prediction error signals elicited by omissions of predicted "what" but not "when". *Front. Hum. Neurosci.* **7**, 407 (2013).
87. L. H. Arnal, V. Wyart, A. L. Giraud, Transitions in neural oscillations reflect prediction errors generated in audiovisual speech. *Nat. Neurosci.* **14**, 797–801 (2011).
88. L. H. Arnal, A. L. Giraud, Cortical oscillations and sensory predictions. *Trends Cogn. Sci.* **16**, 390–398 (2012).
89. R. G. Natan, W. Rao, M. N. Geffen, Cortical interneurons differentially shape frequency tuning following adaptation. *Cell Rep.* **21**, 878–890 (2017).
90. J. M. Ross, J. P. Hamm, Cortical microcircuit mechanisms of mismatch negativity and its underlying subcomponents. *Front. Neural Circuits* **14**, 13 (2020).
91. H. E. M. Den Ouden, J. Daunizeau, J. Roiser, K. J. Friston, K. E. Stephan, Striatal prediction error modulates cortical coupling. *J. Neurosci.* **30**, 3210–3219 (2010).
92. A. M. Bastos, W. M. Usrey, R. A. Adams, G. R. Mangun, P. Fries, K. J. Friston, Canonical microcircuits for predictive coding. *Neuron* **76**, 695–711 (2012).
93. S. Shipp, Neural elements for predictive coding. *Front. Psychol.* **7**, (2016).
94. A. M. H. Lesicko, C. F. Angeloni, J. M. Blackwell, M. De Biasi, M. N. Geffen, Corticofugal regulation of predictive coding. *eLife* **11**, e73289 (2022).
95. A. Bendixen, E. Schröger, W. Ritter, I. Winkler, Regularity extraction from non-adjacent sounds. *Front. Psychol.* **3**, 143 (2012).
96. K. Hara, R. A. Harris, The anesthetic mechanism of urethane: The effects on neurotransmitter-gated ion channels. *Anesth. Analg.* **94**, 313–318 (2002).
97. H. Tsukano, M. Horie, R. Hishida, K. Takahashi, H. Takebayashi, K. Shibuki, Quantitative map of multiple auditory cortical regions with a stereotaxic fine-scale atlas of the mouse brain. *Sci. Rep.* **6**, 22315 (2016).
98. W. Guo, A. R. Chambers, K. N. Darrow, K. E. Hancock, B. G. Shinn-Cunningham, D. B. Polley, Robustness of cortical topography across fields, laminae, anesthetic states, and neurophysiological signal types. *J. Neurosci.* **32**, 9159–9172 (2012).
99. J. Voigts, J. Siegle, D. L. Pritchett, C. I. Moore, The flexDrive: An ultra-light implant for optical control and highly parallel chronic recording of neuronal ensembles in freely moving mice. *Front. Syst. Neurosci.* **7**, 8 (2013).
100. Allen Institute for Brain Science, Allen Reference Atlas. Mouse Brain [brain atlas] (2011); http://atlas.brain-map.org/atlas?atlas=1&plate=100960228#atlas=1&plate=100960069&resolution=8.38&x=6782&y=4142&zoom=-3&z=6.
101. E. M. Trautmann, S. D. Stavisky, S. Lahiri, K. C. Ames, M. T. Kaufman, D. J. O'Shea, S. Vyas, X. Sun, S. I. Ryu, S. Ganguli, K. V. Shenoy, Accurate estimation of neural population dynamics without spike sorting. *Neuron* **103**, 292–308.e4 (2019).

Acknowledgments: We thank Y. Boubenec, F. de Lange, J. L. Peña, B. Shinn-Cunningham, and E. Schröger for comments on a previous version of the manuscript. **Funding:** This work was supported by project PID2019-104570RB-I00 funded by MCIN/AEI/10.13039/501100011033 (to M.S.M.) and Foundation Ramón Areces grant CIVP20A6616 (to M.S.M. and D.P.-G.), European Union's Horizon 2020 grant agreement no. 952378—BrainTwin (to M.S.M., D.P.-G., and A.B.L.-R.), Foundation Ramón Areces grant CIVP20A6616 (to M.S.M. and D.P.-G.), NWO-VIDI grant 016.VIDI.189.052 (to B.E., K.P., and A.A.), NWO-ALW-Open grant (ALWOP-346) (to K.P.), iNavigate grant H2020-MS-CA-RISE-2019-873178 (to E.Y.), and NeurotechEU grant EPP-EUR-UNIV-2020-101004080 (to E.Y.). **Author contributions:** A.B.L.-R. performed experiments in anesthetized rats, data curation and analysis under the guidance of D.P.-G. and M.S.M., and writing—original draft. K.P. performed experiments in the awake mouse and analyzed the data under the guidance of B.E., as well as writing—review and editing. A.A. performed experiments in the awake and anesthetized mouse and contributed to data analysis. E.Y. performed experiments in the anesthetized mouse. D.P.-G. performed conceptualization, software, data curation, formal analysis, and writing—review and editing. B.E. performed conceptualization, supervision, project administration, funding acquisition, contributed to data analysis and writing—review and editing. M.S.M. performed conceptualization, methodology, supervision, project administration, funding acquisition, and writing—original draft, review, and editing. **Competing interests:** The authors declare that they have no competing interests. **Data and materials availability:** All data needed to evaluate the conclusions in the paper are present in the paper and/or the Supplementary Materials.

Submitted 25 June 2022
Accepted 9 May 2023
Published 14 June 2023
10.1126/sciadv.abq8657